Network-based modeling of infectious disease spillover

by

Saswata Das

B.Tech., Maulana Abul Kalam Azad University of Technology,

2018

M.Tech., University of Calcutta, 2021

A THESIS

submitted in partial fulfillment of the
requirements for the degree

MASTER OF SCIENCE

Department of Electrical and Computer Engineering
Carl R. Ice College of Engineering

KANSAS STATE UNIVERSITY
Manhattan, Kansas

2024

Approved by:

Major Professor
Dr. Caterina Scoglio

Copyright

Abstract

This thesis contains two main chapters: Computational Epidemiology (second chapter) and SIR Epidemics in Interconnected Networks: threshold curve and phase transition (third chapter).

In the second chapter, we delve into the basics and history of epidemiology to underscore the importance of understanding zoonotic diseases and the capabilities and limitations of various mathematical modeling approaches. We also discuss various mathematical modeling techniques, such as Agent-Based Modeling, Network-Based Modeling, Patch Modeling, and others.

In the first part of the third chapter, we examine the Susceptible-Infected-Recovered (SIR) dynamics within interconnected networks, emphasizing the structural heterogeneity and interdependencies present in real-world systems. We demonstrate how the epidemic threshold of a contact network is affected when coupled with another network for a fixed infection strength. Our model considers both contact networks and interconnections as generic, depicting the epidemic threshold curve for interconnected networks. We assume that the infection could initially be present in either one or both networks. If the normalized infection strengths exceed the threshold curve, the infection spreads; otherwise, it does not, regardless of the interconnection level.

In the second part of the third chapter, we investigate the spillover phenomenon, where a disease spreads from a reservoir network to a novel host population network. We observe a phase transition when the number of links or

the inter-network infection rate surpasses a specific threshold, keeping other parameters constant. The spillover dynamics reveal two regimes: a major spillover region and a minor spillover region, determined by the fraction of interpopulation links and inter-network infection strength. High spillover probability occurs in the major spillover region, while low probability occurs in the minor region. Additionally, we find that the threshold number of links required to achieve spillover varies with network topology when the number of infected individuals within the reservoir network is nearly equal and the inter-network infection strength is constant.

Overall, this work enhances the understanding of SIR dynamics in interconnected networks and provides insights into the behavior of epidemics in complex systems. It integrates a comprehensive review of computational epidemiology along with significant findings regarding the spread of disease and spillover in interconnected networks.

Table of Contents

Contents

List of Figures . . . . . **vii**

Acknowledgments . . . . . **xii**

Dedication . . . . . **xiii**

Preface . . . . . **xiv**

1 Introduction **1**

2 Computational Epidemiology **3**

2.1 What is Epidemiology 3

2.2 What is Computational Epidemiology 4

2.3 History of Mathematical Modelling of Infectious Disease 7

2.4 What Models Can Do 9

2.5 What Models Cannot Do 12

2.6 Case Study of COVID-19 Mathematical Models: Merits and Limitations 12

2.7 Mathematical Modeling of Zoonotic Diseases 14

2.7.1 Ecological Niche Modeling 18

2.7.2 Patch Modeling 21
2.7.3 Compartmental Modeling 22
2.7.4 Agent-Based Modeling 22
2.8 Network Based Modeling for Epidemics 23
2.8.1 Some Widely Used Network Topologies 26
2.8.2 Some Advantages and Drawbacks of Using Network-Based Models to Simulate Epidemics 28

3 SIR Epidemics in Interconnected Networks: threshold curve and phase transition 30
3.1 Introduction 30
3.2 Background 34
3.3 Modeling SIR spreading in interconnected network 38
3.3.1 Generalized epidemic threshold curve 39
3.3.2 The threshold curve 45
3.4 Modelling Spillover 50
3.4.1 Simulation results 52

4 Conclusions 68
4.1 Abbreviations 70

Bibliography 72

List of Figures

List of Figures

2.1 Elements of computational real-time epidemiology [6]. 6

2.2 History of Epidemic Modeling 8

2.3 Five stages of pathogen emergence from animals to humans [18] . 15

2.4 Ecological Niche Modeling Process [20]. 16

2.5 SIR and SEIR Compartmental Model.β: the transmission rate; γ: the inverse of recovering time; σ: the inverse of incubation period. Dotted lines represent transmission 17

2.6 A network-based model for West Nile disease in USA. Black links are undirected, while orange links are directed [51]. 26

3.1 Schematic of a contact network along with the agent-level stochastic transition diagram for agent i according to the SIR epidemic spreading model. β and δ denote the infection and recovery rate, respectively. The notation a_{ij} is used to represent the connection between agent i and agent j. Specifically, if the value of a_{ij} is 0, it signifies the absence of a link between the two agents. Conversely, if a_{ij} is nonzero, it indicates the presence of a link between agent i and agent j. $I_j(t)$ is the state probability of being infected of node j at time t. 40

3.2 Graph of normalized epidemic threshold τ_{c1}=$\tau_{11,c}$*$\lambda(A_{11})$ as a function of normalized infection strength τ_2=τ_{22}*$\lambda(A_{22})$ with different interconnection levels and α=1. The yellow curve is for a strong level of interconnection (ω=0.2), the red curve is for a medium level of interconnection (ω=0.042), and the blue curve is for a low level of interconnection (ω=0.01). The curve shown in this figure is for the above-mentioned small-world network topology. 46

3.4 Graph of normalized epidemic threshold τ_{c1}=$\tau_{11,c}$*λ(A11) as a function of normalized infection strength τ_2=τ_{22}*λ(A22) with different interconnection level and α=1 for Gilbert networks. The yellow curve is for the high number of interconnections (ω=0.2), the red curve is for a medium number of interconnections (ω=0.042), and the blue curve is for a low number of interconnections (ω=0.01). The network topologies for both networks are Erdos-Renyi. . . . 47

3.5 Graph of normalized epidemic threshold τ_{c1}=$\tau_{11,c}$*λ(A11) as a function of normalized infection strength τ_2=τ_{22}*λ(A22) with different interconnection level and α=1 for Gilbert networks. The yellow curve is for the high number of interconnections (ω=0.2), the red curve is for a medium number of interconnections (ω=0.042), and the blue curve is for a low number of interconnections (ω=0.01). The network topologies for both networks are Erdos-Renyi. . . . 48

3.3 Figures depicting spreading scenarios for weak and strong-level interconnections. The figure shows that when the normalized epidemic strengths are above the threshold, the infection spreads in the contact network (left). When the normalized epidemic strengths are below the threshold, the infection spreads in the contact network (right). 49

3.6 Spillover in networks from reservoir population to the novel host population. 52

3.7 The number of infected agents in novel host population network due to spillover with the fraction of total possible links between novel host population network and reservoir network. Every 16000 realizations have been shown in the boxplot. 55

3.8 Probability of spillover in novel host population network with inter-population link density. All other parameters are kept constant. 56

3.9 The number of infected agents in novel host population network with the inter-network infection rate between novel host population network and reservoir network. Every 16000 realizations have been shown in the boxplot. These boxplots are generated in Matlab 57

3.10 Probability of spillover with inter-network infection rate keeping all other parameters constant. 58

3.11 Spillover region separation based on inter-population links and inter-network infection strength. The green-colored zone is the significant spillover zone, while the yellow zone is the non-significant spillover zone. 59

3.12 The inter-population links are connected with only the hubs of the reservoir network. The spillover size for each fraction of links has been shown in boxplot 60

3.13 The phase transition curve when the inter-population links between novel host population network and reservoir network are connected with the hubs of reservoir network. The phase transition occurs for a very low fraction of links. 61

3.14 SEIR Transition Graph for Ebola Across Interconnected Networks. The diagram illustrates the transition rates between SEIR states, a and h subscript denote to animal and human agents, respectively. Parameters β_{11} and β_{22} represent the infection rates between the agents of the novel host population network and reservoir network, respectively. and β_{12} denotes infection rate between the agents of the reservoir network and novel host population network ; κ_1 and κ_2 indicate the incubation rates of animals and humans respectively that lead to infectious states; δ_1 and δ_2 are the recovery rates of animals and humans respectively. Dashed arrows show the inducing state for transitions. 63

3.15 Illustration of an example for two-layer network structure used in the simulation: (a) represents the contact network among animals, (b) represents the contact network among humans, and the grey arrows denote the directed transmission links from animals to humans. 65

3.16 The boxplot of number of infected agents in novel host population network for the simulation-based study of Ebola. The number of infected agents in the novel host population network increases with the fraction of the possible links between the novel host population network and the reservoir network. 66

3.17 Probability of spillover in host population network for simulation-based study of Ebola 66

Acknowledgments

I extend my heartfelt gratitude to everyone who has supported and assisted us in the completion of this thesis. First and foremost, I am deeply thankful to Dr. Caterina Scoglio for her invaluable guidance, effort, and time throughout the master's program, which has been instrumental in shaping this research. I am also grateful to the members of the Network Science and Engineering Lab (NetSE) for their unwavering support and assistance. Additionally, I sincerely thank my parents, friends, other professors, and the non-teaching staff of Kansas State University for their immense support over these past two years in my pursuit of a Master of Science degree.

Dedication

I dedicate this thesis to my parents, whose unwavering love and support have been my greatest source of strength and inspiration. To my teachers, whose wisdom and guidance have illuminated my path and nurtured my academic growth. And to my friends, whose encouragement and camaraderie have made this journey both enjoyable and fulfilling. Thank you all for being my pillars of support and for believing in me every step of the way.

Preface

This thesis represents the culmination of my research in the Master's program in Network Science and Engineering at Kansas State University. It consists of two main chapters that explore distinct yet interconnected aspects of mathematical modeling in epidemiology using network science.

Chapter 2 introduces epidemiology, tracing its historical development in mathematical modeling, and discusses the significance and limitations of various model types used in describing epidemics. It also delves into the specialized area of zoonotic disease modeling, an essential subfield within epidemiology.

Chapter 3 focuses on the application of network-based models in epidemiology. The first part examines how the epidemic threshold of a contact network changes when coupled with another network under a fixed infection strength. The second part investigates the impact of the number of interpopulation links on the size of the infected population within a host network.

Throughout this thesis, I have aimed to provide a thorough analysis of mathematical modeling in epidemiology, aiming to contribute meaningfully to the ongoing discourse in this field. Each chapter reflects extensive research, critical analysis, and scholarly inquiry.

I extend my heartfelt gratitude to my thesis advisor, Dr. Caterina Scoglio, whose guidance and expertise have been pivotal in shaping this thesis. Her insightful feedback and unwavering support have been invaluable throughout

my academic journey.

I am also thankful to the members of the Network Science and Engineering group for their contributions and encouragement, which enriched the development of this thesis.

Lastly, I am deeply grateful to my family and friends for their unwavering support, understanding, and encouragement during the challenging yet rewarding process of completing this thesis.

It is my sincere hope that this thesis makes a significant contribution to network science and inspires further research and exploration in this important area of study.

Chapter three of this thesis is based on a scientific paper I wrote, which has been accepted for publication in the Applied Network Science Journal [1].

Saswata Das

07/22/2024

Chapter 1

Introduction

My thesis comprises two main chapters: Chapter 2 focuses on Computational Epidemiology, while Chapter 3 explores SIR Epidemics in Interconnected Networks, specifically addressing the threshold curve and phase transition phenomena. Chapter 1 serves as the Introduction, and Chapter 4 concludes the thesis.

In Chapter 2, we extensively cover key aspects of computational epidemiology. Starting with the definitions of epidemiology and computational epidemiology, we progress to examining the historical evolution of mathematical modeling and its capabilities. The chapter also addresses the modeling of zoonotic diseases, explores various modeling approaches, and concludes with an in-depth discussion on network-based modeling for epidemics.

In Chapter 3, we conducted research on SIR epidemics in interconnected networks. In the first part, we demonstrate that the interconnection between two networks can facilitate disease spread in both, even when the infection strength

in each network is below its epidemic threshold. We plotted three distinct epidemic threshold curves for weak, medium, and strong coupling. Our findings indicate that despite SIR dynamics suggesting lower epidemic thresholds compared to individual networks, infections can persist across the interconnected system. In the second part of the chapter, we focused on spillover dynamics and showed that a clear phase transition in the probability of spillover consistently occurs with an increase in the number of interpopulation links, regardless of whether humans act as dead-end hosts. We also presented phase transition curves for interpopulation links and inter-network infection rates, delineating major and minor spillover areas based on these factors. Our network-based models are built upon the contexts of the West Nile virus, Avian influenza, and Ebola disease.

The main contributions of my thesis are:

- A comprehensive discussion about computational epidemiology.
- The determination of an epidemic threshold curve for SIR spreading in interconnected networks.
- The discovery of a phase transition for spillover as a function of the level of interconnection.
- The determination of a major or minor spillover probability region as a function of the level of interconnection and inter-network infection strength.

Chapter 2

Computational Epidemiology

2.1 What is Epidemiology

Epidemiology originates from the Greek terms "epi," "demo," and "logy," which translate to "upon," "the common people," and "study," respectively. Together, these words form the concept of "the study of what befalls the common people." Today, epidemiology is defined as studying the distribution and determinants of disease frequency in human populations and applying this knowledge to manage and control health issues [2]. David Lilienfeld was an American epidemiologist known for his work; in 1978, David Lilienfeld published a paper on definitions of epidemiology [3]. He proposed the definition of epidemiology as follows: *"Epidemiology is a method of reasoning about a disease that deals with biological inference derived from observations of disease phenomena in popula-*

tion groups.". Here, we can include another definition of epidemiology given by another epidemiologist, Alfred S Evans *"Epidemiology is the quantitative analysis of the circumstances under which disease processes, including trauma, occur in population groups, factors affecting their incidence, distribution, and the host response and use of this knowledge in prevention and control"* [4]. Frerot et al. have done a very good review of the definitions of epidemiology and how they changed from 1978 to 2017 [5].

2.2 What is Computational Epidemiology

Computational epidemiology is an interdisciplinary field focused on developing and utilizing computer models to understand and control the spatiotemporal diffusion of diseases through populations. These models range from descriptive, such as static estimates of correlations within large databases, to generative, like computing the spread of disease through person-to-person interactions in large populations. The scope of diseases studied includes not only infectious diseases but also more general reaction-diffusion processes, like the diffusion of innovation. The populations of interest vary with the disease, encompassing humans, animals, plants, and even computers. Correspondingly, the interactions modeled depend on the nature of the disease, from physical proximity in aerosol-borne diseases to sexual contact in sexually transmitted infections and insect-feeding patterns in mosquito-borne illnesses.

Computational models play a crucial role in understanding the space-time dynamics of epidemics. They are instrumental in evaluating various intervention strategies, including pharmaceutical interventions like vaccinations and antivi-

rals, as well as non-pharmaceutical measures such as social distancing and school closures. Individual behavior and public policies are critical factors in managing epidemics, and computational techniques offer powerful tools for studying these aspects.

In pervasive computational environments, analysts can access real-time models, data, and expert opinions as an epidemic unfolds. The development of computational methods and approaches needs to occur within a multidisciplinary context. For example, specific inference methods should be developed in collaboration with statisticians and biologists. Addressing issues like vaccine production, allocation, and usage requires input from social, economic, and behavioral scientists to ensure efficient and equitable use while considering social and economic factors. Additionally, user interfaces and decision-support environments must be created in conjunction with psychologists and statisticians to avoid biases in human judgment.

Computational epidemiology thus represents a vital, multifaceted approach to understanding and combating the spread of diseases. It integrates knowledge and techniques from diverse fields to inform and enhance public health strategies.

Figure 2.1 in the thesis depicts a thorough computational approach to real-time epidemiology, encompassing the five key areas identified by Fineberg and Wilson. The five key areas where science can support real-time epidemiology, as identified by Fineberg and Wilson, are pandemic risk, vulnerable populations, available interventions, implementation possibilities, shortcomings, and public understanding. This holistic perspective demonstrates how computational tools

and models can effectively assist in comprehending and managing epidemics [6].

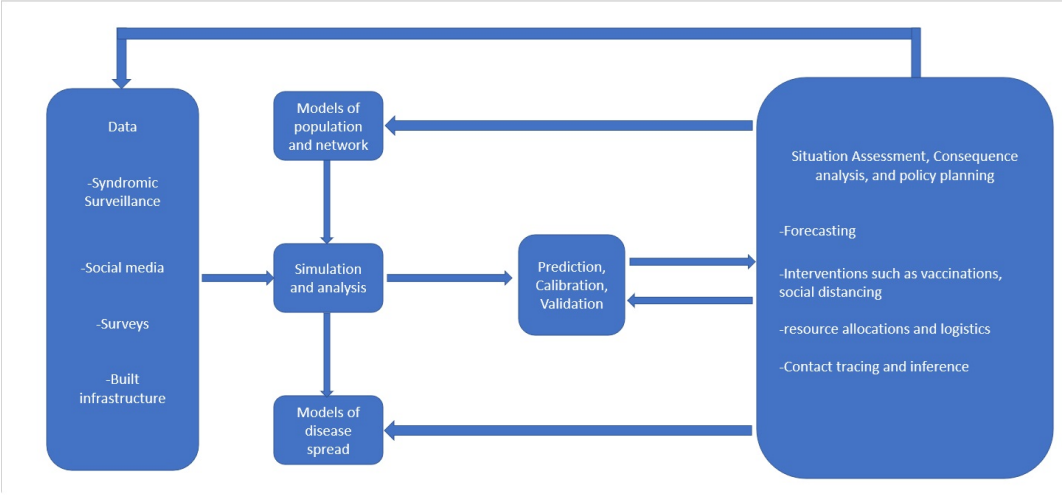

Figure 2.1: Elements of computational real-time epidemiology [6].

2.3 History of Mathematical Modelling of Infectious Disease

Scientists developed different models to limit the extent of disease spread and predict various aspects of an outbreak. One of the first individuals to explain disease through mathematical modeling was John Graunt, who performed his studies in London at the time of King Charles II. Grunt published his work in his book Natural and Political Observations Made upon the Bills of Mortality" [7]. The Bills of Mortality were weekly records documenting the number and causes of deaths in London parishes. These records started in 1592 and have been maintained without interruption since 1603. John Graunt utilized this data to analyze different causes of death and developed a method to estimate the relative risks of dying from various diseases, laying the groundwork for the theory of competing risks.

Later, in 1766, Daniel Bernoulli contributed to the field of epidemiology. In the eighteenth century, smallpox was endemic. To fight it, variolation, a form of inoculation with a milder strain, was introduced. It aimed to provide lifelong immunity but carried a risk of infection and even death. There was a debate among scientists regarding the effectiveness of variolation, and Bernoulli was led to study this question. Some remarkable works of Bernoulli are cited in my thesis [8, 9, 10].

Thomas Robert Malthus developed the Malthusian growth model in 1798, which posits that population growth is exponential while food supply growth is linear, leading to eventual overpopulation and resource scarcity [11]. In 1825,

Benjamin Gompertz introduced the Gompertz model, a type of mathematical model for a time series, where growth is slowest at the start and end of a time period [12]. Pierre-Francois Verhulst formulated a logistic equation for population growth between 1838 and 1847, providing a more realistic model of population dynamics that includes a carrying capacity. Another systematic and data-driven investigation of the spread of epidemics was conducted by John Snow, a British physician, who analyzed a cholera outbreak in London in 1854. In the early 1900s, Anderson, Gray, McKendrick, and William Kermack further advanced the development of mathematical models for infectious diseases by developing the compartmental model for infectious diseases [13] [14, 6, 15].

Below, we show the history of mathematical modeling of infectious diseases using a diagram shown in figure 2.2.

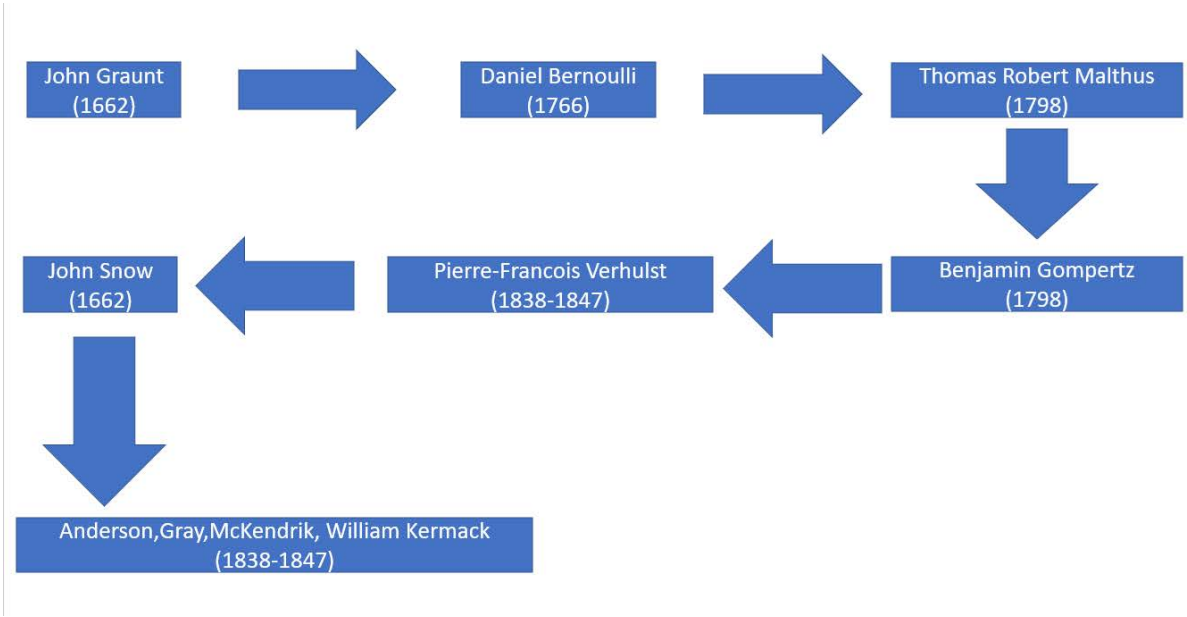

Figure 2.2: History of Epidemic Modeling

2.4 What Models Can Do

Models play two critical roles in the study of epidemiology: prediction and understanding. These roles are often intertwined with the model properties of accuracy and transparency, which can sometimes be in conflict. Predictive models typically demand a high degree of accuracy to include all known complexities and population-level heterogeneities. In contrast, models aimed at improving understanding prioritize transparency, allowing for a clearer insight into the underlying mechanisms of disease spread.

Prediction is the most obvious and widely recognized use of models. It involves making the models as accurate as possible by incorporating all complexities and heterogeneities at the population level. Accurate predictive models are especially powerful in guiding policy decisions, particularly when there are trade-offs between different control strategies.

For instance, during the 2001 UK foot-and-mouth epidemic, models were essential in addressing two primary questions: whether the epidemic was under control and whether additional targeted culling would reduce livestock loss. Three distinct models, each based on different assumptions about the disease's dynamics, were used. Despite their differences, all models provided similar advice: predicting a large-scale epidemic and recommending additional, locally targeted culling to dramatically reduce the number of cases and the overall loss of livestock.

Similarly, predictive models were crucial in evaluating the control of potential bio-terrorist releases of smallpox. The main question here was whether to employ mass vaccination or targeted measures. While mass vaccination is gen-

erally effective against large outbreaks, it could cause more health issues than a small-scale epidemic due to the side effects of the vaccine. Models ranging from simple to highly complex were used, but they offered conflicting advice due to uncertainties in epidemiological parameters and different underlying assumptions. The optimal conditions for mass vaccination against smallpox remain an open question.

Accurate predictive models also serve as valuable statistical tools. They can signal deviations from normal epidemic behavior, acting as diagnostic warnings. For example, while isolated meningitis cases may be typical, a cluster of cases might indicate the start of a localized epidemic, prompting immediate action based on the model's predictions. During eradication campaigns, models can detect regions not responding as predicted, targeting them for more intensive control measures. Additionally, detailed modeling and robust statistical analysis of reported and hospitalized cases can help identify the early emergence of an epidemic.

Models are equally important for understanding how infectious diseases spread in the real world and how various complexities affect their dynamics. They provide epidemiologists with an idealized framework where individual factors can be examined in isolation, and every facet of disease spread is recorded in perfect detail. This allows for the examination of a range of issues in a robust and generic framework. For example, models can study the effects of variable numbers of sexual partners on the spread of sexually transmitted diseases, increased transmission among children during school terms, or the localized spread of infection.

While these modeling approaches might seem driven purely by scientific curiosity, they often yield insights that are both robust and generic, applicable to a wide variety of problems. The understanding gained from such modeling helps develop more sophisticated predictive models and gather relevant epidemiological data, allowing researchers to determine which elements are essential and which can be neglected. By building an intuition for infection patterns and progressively developing from simple to more complex models, researchers can begin to comprehend the rich complexities and dynamics observed in the real world.

In summary, models in epidemiology serve two primary roles: predicting the course of diseases and enhancing our understanding of disease dynamics. Predictive models guide policy decisions and serve as diagnostic tools, while models focused on understanding provide insights into the factors influencing disease spread. Both types of models are crucial for advancing our knowledge and management of infectious diseases, highlighting the interplay between accuracy and transparency in modeling efforts [16].

In addition to their roles in prediction and understanding, models are also crucial in formulating effective mitigation strategies for diseases. By simulating various intervention scenarios, models can help identify the most effective measures to reduce transmission, minimize impact, and allocate resources efficiently. For instance, during an outbreak, models can evaluate the potential outcomes of strategies such as social distancing, vaccination campaigns, and travel restrictions. By comparing different approaches, models can guide public health officials in choosing the best course of action to mitigate the spread of

disease. This ability to test and refine intervention strategies in a virtual setting is invaluable, especially when dealing with new or emerging infectious threats where real-world experimentation is not feasible or ethical.

2.5 What Models Cannot Do

Models have inherent limitations. Achieving a fully accurate model is impossible; there will always be aspects of host behavior or disease quirks that remain unknown or unknowable. For instance, creating an accurate model for a human airborne infection, such as influenza, would require accounting for variations in transmission due to temperature and climate, tracking daily movements and interactions of individuals, and considering the variability in susceptibility caused by genetic factors or past infections. Even if such a comprehensive model were possible, the random nature of transmission would still prevent perfect predictions. We will never be able to forecast the precise course of an epidemic or identify exactly which individuals will be infected. The best we can achieve are models that offer confidence intervals on epidemic behavior and assess the risk of infection for different groups of hosts [16].

2.6 Case Study of COVID-19 Mathematical Models: Merits and Limitations

In this section, I aim to illustrate the limits and merits of mathematical models by providing a real-time example, drawing on insights from the review article by Afzal et al. [17].

As per the authors, the merits of mathematical models are significant in the realm of epidemiology. These models enable countries to proactively prepare for preventing widespread epidemics and managing unforeseen healthcare system demands. They assist authorities in gauging the effectiveness of lockdown measures and deciding when to implement stringent, partial, or relaxed measures based on the virus's reproduction and incubation rates. Moreover, mathematical models are essential for estimating transmission parameters and planning pandemic responses despite inherent uncertainties. They provide a clear understanding of the epidemic's dynamics and help forecast its propagation. Furthermore, mathematical models navigate the delicate balance between the need for social distancing to prevent the pandemic and the necessity of social interaction for economic sustainability, facilitating a balanced long-term strategy.

According to the authors, mathematical modeling in epidemiology also presents several limitations. Decision-makers and authorities may only find the information from mathematical modeling results or predictions useful if they fully comprehend the impact of the underlying assumptions. The vast volume and rapid evolution of published COVID-19 literature contribute to research findings and guidelines constantly changing with new data. Furthermore, reported treatment outcomes often rely heavily on observational or limited clinical studies, raising concerns about bias and imprecision in assessing treatment effectiveness. Additionally, limitations in the analysis, such as focusing exclusively on adult patients, mean the results may not apply to pediatric populations. Language barriers also restrict the scope of research articles, as studies are primarily based on English publications or translations, potentially overlooking valuable foreign knowledge. Moreover, simplifications in mathematical modeling and data fitting, such as fixed transmission rates, may not accurately reflect real-world variability influenced by epidemiological, socioeconomic factors, and outbreak control measures. Nobel Laureate Robert Solow emphasized that for mathematical modeling to be successful and useful, it must be simplified, executed correctly, and rendered plausible.

2.7 Mathematical Modeling of Zoonotic Diseases

From the above discussion, it is clear that mathematical modeling is a crucial tool for predicting diseases. In the context of zoonotic disease modeling, there is a need for enhanced computational focus on the interconnected dynamics of human and wildlife systems that drive the emergence of zoonotic diseases.

Additionally, it is essential to incorporate the inherent heterogeneities within these systems. The complexity of these interactions is likely the most significant obstacle to comprehending spillover dynamics and managing the emergence of potential zoonotic diseases. Pike et al. outlined a zoonotic disease emergence model that describes the five stages of pathogen emergence from animals to humans [18] 2.3. Alexander et al. have reviewed various mathematical models that are useful in predicting any zoonotic disease [19].

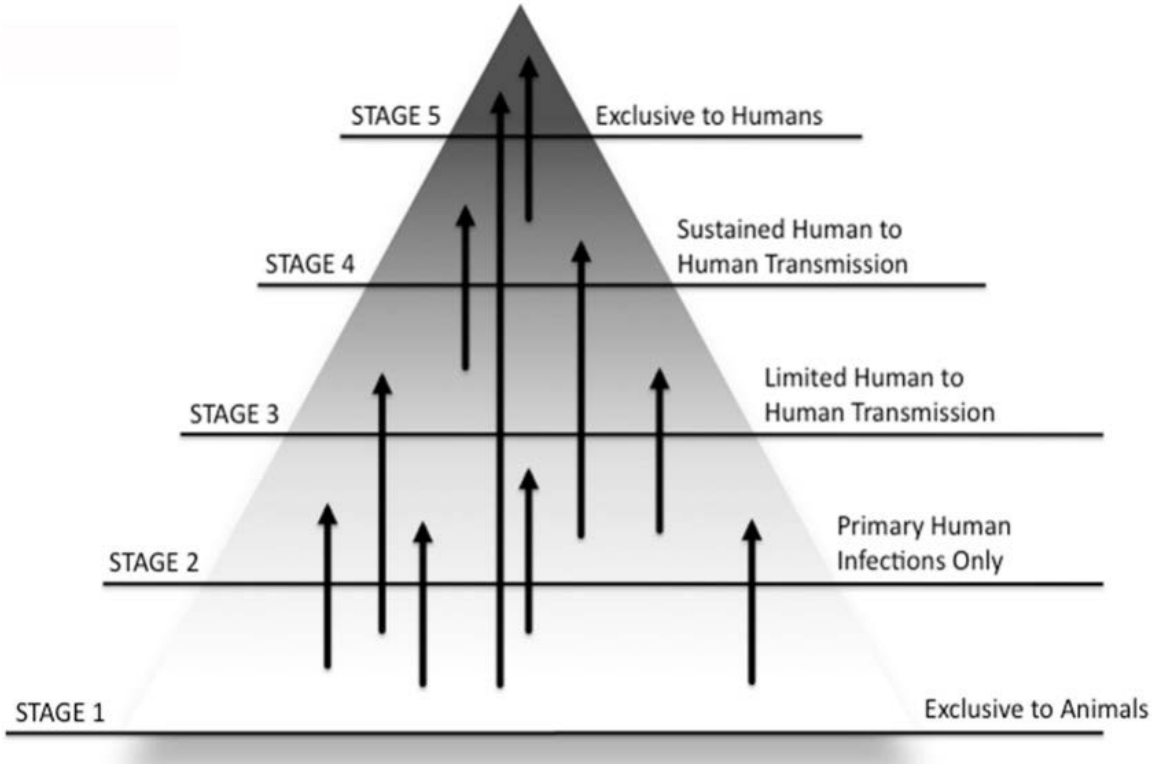

Figure 2.3: Five stages of pathogen emergence from animals to humans [18]

One method is ecological niche modeling, particularly predictive ecological niche modeling (ENM), which is extensively utilized to forecast the geographic distribution of various zoonotic pathogens and parasites and analyze and determine the key factors linked to outbreaks. In Figure 2.4, the process of ENM is shown [20] . Ecological niche modeling can serve as a crucial initial step in comprehending the geographic potential of a disease. This can be achieved either by modeling the pathogen itself (e.g., Bacillus anthracis) or the broader system (e.g., Ebola). Niche-based predictions can guide other modeling approaches and delineate the multivariate space where zoonoses and spillover events are most probable. By projecting onto unexplored landscapes or future time periods, modelers can make predictions about wider geographic areas or the impacts of climate change.

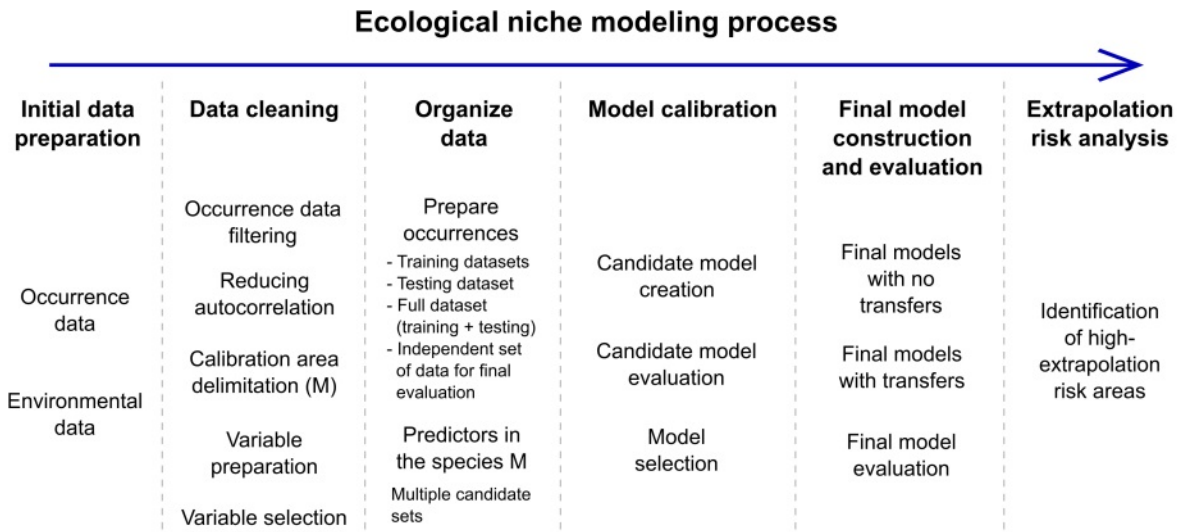

Figure 2.4: Ecological Niche Modeling Process [20].

Compartmental modeling plays a significant role in mathematical epidemiology. This approach involves dividing the entire population into different compartments based on disease states, such as Susceptible, Exposed, Infected, Recovered, and Vaccinated. These compartments are represented by equations that describe the system and require parameters to represent the interactions between different compartments. Some popular compartmental models frequently used for the purpose of mathematical modeling of epidemics are SIR Model: Susceptible-Infected-Recovered, SIS Model: Susceptible-Infected-Susceptible, SEIR Model: Susceptible-Exposed-Infected-Recovered, SEIV Model: Susceptible-Exposed-Infected-Vaccinated, etc. Below, in figure 2.6, we present the compartmental models for SIR and SEIR.

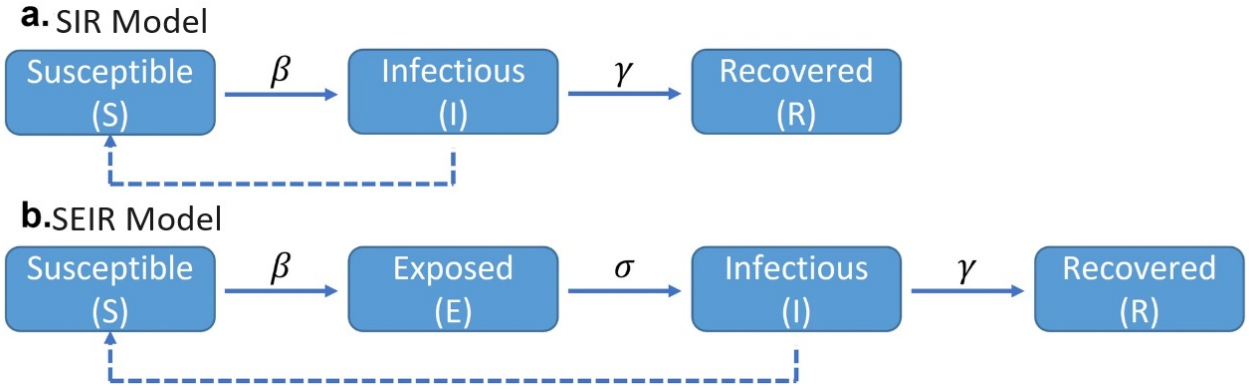

Figure 2.5: SIR and SEIR Compartmental Model.β: the transmission rate; γ: the inverse of recovering time; σ: the inverse of incubation period. Dotted lines represent transmission

Patch modeling, or metapopulation modeling, extends compartmental models used to represent populations across different locations or "patches." Each patch has unique characteristics related to the environment, pathogens, or host populations. By dividing a large area into these distinct patches, the model can account for variations and interactions between patches, providing a more detailed and realistic understanding of how diseases or other factors spread and interact across different geographical areas.

Agent-based modeling is another widely utilized approach for describing epidemic spread. This model comprises agents, their environment, and the rules governing their behavior. Agents can be richly characterized with diverse attributes, and multiple classes of agents can be established. Agent-based models can accommodate highly complex dynamics, as the interaction rules for each agent can depend on the current states of other dynamic processes. However, it can be concluded that greater model complexity and higher data resolution do not necessarily guarantee high-quality results. As individual characteristics increasingly diverge from population-level patterns, the modeling requirements become more complex.

2.7.1 Ecological Niche Modeling

Lawrence et al. conducted a systematic review to shed light on the current state of the science and practice of using ecological niche modeling to predict the emergence and spread of vector-borne and zoonotic diseases [21]. The authors screened 383 articles at the abstract level and 237 articles at the full-text level. However, the authors concluded that ENM-based studies to predict

vector-borne and zoonotic diseases have been unevenly distributed across various journal fields. This indicates a need for increased engagement with environmental and veterinary sciences to provide greater insight into the biotic factors contributing to disease emergence. The distribution of these studies is uneven across geographic regions, not only across journal fields. Most of the studies are conducted in less developed tropical countries where the chance of disease emergence is high and the infrastructure to fight epidemics is low. So, conducting these studies is very important in those places where diseases are most vulnerable to emergence. Regarding the effectiveness of these studies, the authors have said that the studies that focus solely on the abiotic and mobility factors or on biotic and mobility factors might not support the long-term persistence of disease for various reasons. A stable population of host species can be found in regions where the Ecological Niche Model considers both biological, environmental, and mobility factors. For the pitfalls identified in these studies, the authors have noted potential challenges associated with using MaxEnt (Maximum Entropy) or GARP (Genetic Algorithm for Rule-set Prediction). While the AUC (Area Under Curve) of the ROC (Receiver Operating Characteristics) is commonly used for model performance evaluation, it has also faced criticism. There is an emphasis on incorporating diverse abiotic, biotic, and especially social factors to enhance model performance.

Li et al. utilized ecological niche modeling to forecast the potential distribution of scrub typhus in Fujian Province by analyzing occurrence data and various risk factors [22]. Their efforts included developing a risk map to assist public authorities in identifying high-risk populations and predicting the

disease's spread. Nayakarahuka et al. conducted ecological niche modeling for Filoviruses, creating a risk map tool to predict the spread of Ebola and Marburg Virus Disease outbreaks in Uganda [23]. Using the MaxEnt (Maximum Entropy) method, they found that temperature and rainfall seasonality were the most significant environmental factors in their spatial prediction model for these viruses. Xu et al. employed Geographic Information Systems (GIS) and ecological niche modeling (ENM) to rigorously examine the connections between the occurrence of H7N9 and significant environmental factors, including meteorological variables, human population density, bird migratory routes, wetland distribution, and locations such as live poultry farms, markets, and processing factories [24]. Using the process of ecological niche modeling, an ensemble ecological niche model for West Nile virus habitat prediction in the state of Florida was developed by Beeman et al. [25]. Assefa et al. used an Ecological Niche Model (ENM) to map the global suitability of AHSv (African Horse Sickness viruses) using historical outbreak data from 2005 to 2019 [26]. The Maxent ecological niche modeling program was employed by Millet et al. to predict the distribution of *Culex tritaeniorhynchus* in Asia, the primary vector of Japanese encephalitis virus (JEV) [27]. The study of Li et al. aims to pinpoint high-risk areas for dengue fever outbreaks in the Pearl River Delta (located in southern China), analyze influencing factors using an ecological niche model (ENM), and provide insights for disease prevention and control in the region [28]. The study done by Monroe at al. uses ecological niche modeling (ENM) to identify regions in tropical Africa that are suitable for the occurrence of human Tanapox and to identify potential reservoirs [29].In this study of Sallam et al., ecological

niche modeling was utilized to create a practical map indicating suitable habitats for potential infective mosquito vectors of West Nile Virus (WNV) in St. John's County of Florida [30]. Richman et al. ecological niche modeling was employed to predict the distribution of seven mosquito vectors of Chikungunya virus across two consecutive rainy seasons in Kédougou, Senegal, using Maxent [31].

2.7.2 Patch Modeling

Choi et al. have proposed a patch model suitable for modeling influenza epidemics in Korea. In their patch model, they divided the whole country into 16 separate regions and accounted for the interactions between these 16 patches [32]. Rebaza et al. have developed a multipatch model for Ebola Virus Disease. While their primary focus is on studying Ebola, their model is adaptable and can be modified to investigate other diseases, such as COVID-19 [33]. Zhang et al. have proposed a multipatch model for West Nile Virus disease. The study demonstrates that the movement of birds between patches is adequate to sustain the persistence of the West Nile virus within each patch [34]. Chen et al. examined how dog movement influences the spread of rabies between provinces in Mainland China using a multipatch model. They found that the migration of dogs between provinces can lead to the disease becoming endemic, even if rabies would otherwise die out within isolated provinces without such migration [35]. Maliyoni et al. explored tick-borne disease dynamics using patch modeling, examining how host and tick migration between geographical patches impact disease persistence and control strategies [36].

2.7.3 Compartmental Modeling

Wonham et al. developed an eight-compartmental model, extending the classical SIR model, to describe West Nile virus cross-infection dynamics over one season [37]. Bekoe et al. developed a compartmental model to simulate the 2014 Ebola Virus Disease outbreak in Guinea, showing how interventions can reduce the epidemic's spread and potential to die out [38]. Lee et al. developed a compartmental model with a vector-host structure to analyze Zika virus dynamics and evaluate containment strategies. The model helps decision-makers by providing insights on minimizing infections and emphasizes the role of digital disease surveillance [39]. Danzetta et al. review recent studies that develop compartmental models to understand Rift Valley fever virus (RVFV) transmission dynamics. The review section includes references, study area, period, type of model, compartments, climatic variables, outcomes, objectives, and key results for each paper [40]. Malek et al. developed a deterministic six-compartment model to illustrate the progression of bird flu in poultry, including individual epidemiological statuses and intervention measures. Their SEIATR mathematical model for bird flu is an adaptation of the SEIR compartmental model specifically tailored for poultry farm settings [41].

2.7.4 Agent-Based Modeling

Stiner et al. developed an agent-based model in NetLogo to simulate West Nile Virus transmission via mosquitoes, humans, horses, and birds, assessing vaccination impacts and public health interventions. The model aims to guide horse vaccination strategies and illustrate the role of public health efforts in

controlling human infections [42]. Siettos et al. have created an agent-based model to study the epidemic dynamics of Ebola virus disease (EVD) in Liberia and Sierra Leone from May 27 to December 21, 2014 [43]. Kuhlman et al. introduce a hybrid agent-based model capable of scaling to millions of human agents and mosquitoes, applied to simulate the Zika outbreak in the Fall of 2016 among a synthetic population of 1.2 million individuals in Miami, Florida, USA [44]. Nguyen et al. utilize the estimated global transmission rate to construct a simulation model using agent-based modeling aimed at studying fundamental aspects of the avian influenza epidemic in poultry and evaluating potential effective measures to mitigate its outbreak [45]. Huang et al. employed Agent-Based Modeling (ABM) to construct a model for simulating and evaluating various control strategies against *Echinococcus granulosus*. These strategies encompassed interventions such as dosing dogs, regulating livestock slaughter, health education, vaccinating intermediate and definitive hosts, administering slow-released praziquantel injections to dogs, and reducing the dog population [46].

2.8 Network Based Modeling for Epidemics

Early epidemiological models were based on the assumption of random mixing across the entire population. However, in reality, each person has a limited number of contacts to whom they can transmit infection, creating a 'mixing network' that consists of all these individual connections [47]. The number of contacts for each agent can vary significantly, which can be accurately modeled in a network-based modeling approach. For example, in a scale-free network, hubs contain more links compared to other nodes.

In epidemics, it is often noted that a small number of "superspreaders" transmit the infection to many others, while most infected individuals either do not spread the infection or pass it to very few people. This observation indicates that assuming homogeneous mixing at the start of an epidemic may not be accurate [48].

We can represent the network of contacts between individuals using a graph, where members of the population are vertices, and the contacts between them, which can transmit infection, are edges. Contacts do not necessarily transmit infection. For each contact between individuals of whom one has been infected and the other is susceptible, there is a probability that infection will actually be transmitted. This probability depends on such factors as the closeness of the contact, the infectivity of the member who has been infected, and the susceptibility of the susceptible member [48].

There are various simulation processes to simulate epidemics over a contact network. Here, we are discussing the simulation methodology proposed by Sahneh et al. [49, 50].

Several steps are required to simulate a disease using a network-based model. First, we need to formulate a contact network. Next, we define which nodes are initially infected in this network. We also specify the number of compartments and the various rates of disease spreading.

For example, in the SIS model, each individual can be either "susceptible" or "infected," resulting in two compartments. A susceptible individual can become infected if they are in contact with infected individuals. The infection process for an individual with one infected neighbor follows a Poisson process

with a transition rate of β. These infection processes are stochastically independent. Therefore, for a susceptible individual with multiple infected neighbors, the transition rate is the infection rate multiplied by the number of infected neighbors. There are two types of transition rates: node-based and edge-based. A node-based transition, or nodal transition, refers to a process that occurs independently of the states of other nodes (or agents) in a network. An edge-based transition refers to a process that occurs as a result of the interaction between a pair of agents (nodes) connected by an edge in a network. For example, in the SIS model, when a susceptible agent becomes infected with an infection rate β, it is an edge-based transition, but when an infected agent is cured with a cure rate of δ, it is a node-based transition. Therefore, we need to define the number of compartments, such as 2 for the SIS model, 3 for the SIR model, and 4 for the SEIR model. We also need to define various rates and the initial status of infected individuals. Then, we can simulate the epidemic process. In the figure below, we can see a network-based model done by Moon et al., to model the West Nile Virus disease in the USA [51]. In this modeling approach, birds are considered as links represent nodes of the network, and mosquito density.

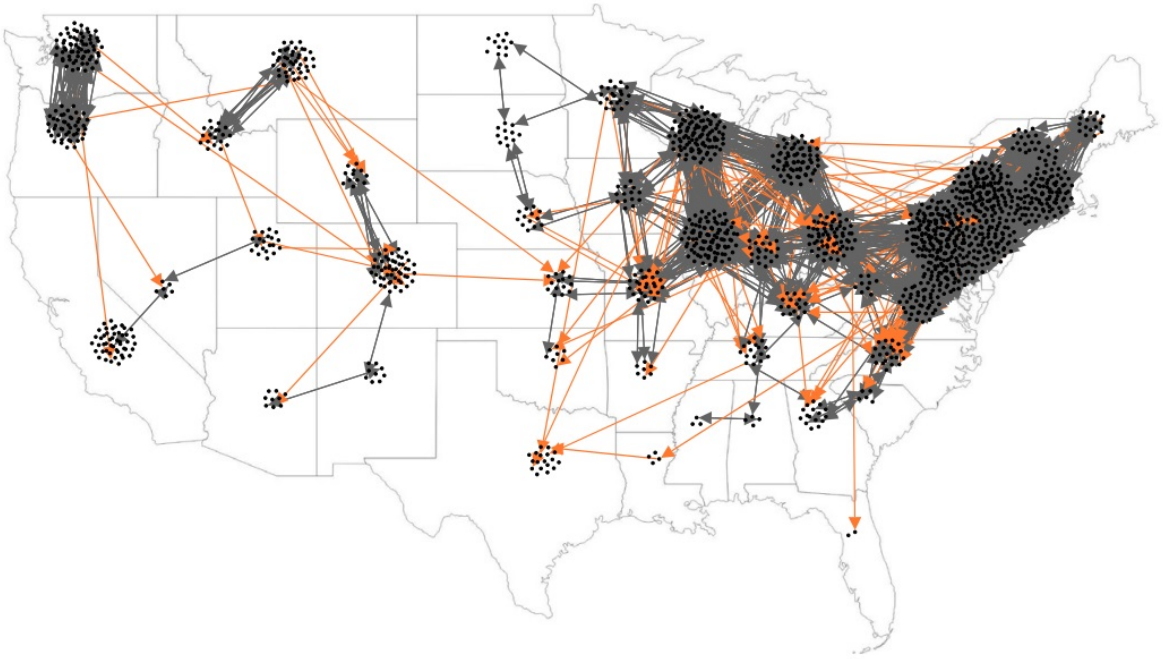

Figure 2.6: A network-based model for West Nile disease in USA. Black links are undirected, while orange links are directed [51].

2.8.1 Some Widely Used Network Topologies

1. Regular Lattice Network: A regular lattice network is structured in a grid-like pattern where each node is connected to its nearest neighbors in a consistent and predictable manner. This topology is characterized by nodes having an equal number of connections (degree) and a uniform distance between neighboring nodes. Regular lattices are often used in modeling physical and biological systems due to their simplicity and the ease with which spatial relationships can be analyzed.

2. Erdos-Renyi Model: The Erdős-Rényi model is a random graph model where each pair of N nodes is connected with a fixed probability p. It is characterized by its uniform edge probability across all node pairs, making it a fundamental tool in theoretical studies of random graphs and a benchmark for understanding network properties in various disciplines.

3.Watts-Strogatz Model : The Watts-Strogatz model generates networks with small-world properties by starting with a regular lattice and randomly rewiring edges with a rewiring probability p. This process creates graphs that combine high clustering coefficients with short average path lengths, mimicking real-world networks such as social or biological systems.

4.Barabasi-Albert Model : The Barabási-Albert model generates scale-free networks using a preferential attachment mechanism, where new nodes are more likely to connect to existing nodes with higher degrees. This results in a network with a power-law degree distribution, mimicking many real-world networks like the Internet and social networks.

2.8.2 Some Advantages and Drawbacks of Using Network-Based Models to Simulate Epidemics

Network-based models have been very successful in epidemiology and can capture the heterogeneous mixing of populations, they also have distinct advantages. These models allow for the simulation of realistic contact patterns among individuals, reflecting the complex social structures that influence disease transmission. Moreover, they can elucidate the role of highly connected individuals (hubs) in spreading infections, offering insights into targeted intervention strategies. Additionally, network-based approaches facilitate the study of disease spread in dynamic populations and across geographic regions, providing a nuanced understanding of epidemic dynamics that traditional compartmental models may overlook. By simulating various mitigation strategies such as targeted isolation or travel restrictions within networks, these models can guide public health interventions to mitigate the impact of outbreaks more effectively. However, network-based modeling does have several drawbacks, including challenges in data collection, defining meaningful contacts, and the need for disease-specific networks, which complicate their practical application [47].

1. Data Collection Challenges: Determining a complete mixing network requires extensive data on every individual and their relationships, which is impractical for large populations due to the volume of data and the issues with recall and willingness to share personal information, especially in sensitive contexts like sexual networks.

2. Defining Network Links: There's a fundamental challenge in defining what constitutes a meaningful contact for transmission. The amount of contact required for infection can vary greatly between diseases, making it difficult to establish consistent and accurate criteria for network links.

3. Disease-Specific Networks: Different diseases spread through different types of contact, meaning that each disease requires its own specific network model. This complicates the process and requires tailored data collection and analysis protocols for each disease.

4. Complexity of Weighted Networks: While considering valued (weighted) networks can provide more accurate models by reflecting the strength of connections, this approach significantly increases data collection challenges and the complexity of the models, making it impractical for all but the simplest cases.

5. Dependence on Assumptions and Protocols: The accuracy of the networks and the insights derived from them are highly dependent on the assumptions and protocols used during data collection. This introduces a level of subjectivity and potential bias into the models.

Chapter 3

SIR Epidemics in Interconnected Networks: threshold curve and phase transition

3.1 Introduction

Various types of contagious diseases are found all over the world. It is crucial to prevent the spread of these diseases. Consequently, extensive research is being conducted to halt their transmission. In addition to other research endeavors, scientists are also crafting diverse mathematical models. These models can aid in understanding disease-spreading mechanisms, estimating potential outbreak sizes, and formulating more effective mitigation strategies.

Considerable progress has been made in the realm of mathematical research on epidemic diseases, encompassing both theoretical and practical applications. Numerous epidemic models are formulated as dynamical systems of ordinary differential equations. Delay differential equations have demonstrated their efficacy in capturing the variability observed in infectious periods within diverse epidemic models. Furthermore, incorporating factors like age structure and spatial considerations has contributed to the development of partial differential equations [52].

Compartmental models are also very useful for studying epidemic diseases. These models for epidemics are of different types, such as the SIS (Susceptible-Infected-Susceptible) model, the SIR (Susceptible-Infected-Recovered) model, and the SEIR (Susceptible-Exposed-Infected-Recovered) model, among others [53]. In the SIR model, infected agents recover and become permanently immune, never becoming infected again. The SIR model is particularly effective in explaining diseases like influenza, COVID-19, and other contagious diseases.

Many epidemiological models simplify the assumptions regarding the patterns of disease-causing interactions among hosts. Specifically, in homogeneous-mixing models, it is assumed that hosts have identical rates of disease-causing contact. In recent years, several network-based approaches have been developed to explicitly model the heterogeneity in host contact patterns [54].

A contact network plays a crucial role in facilitating the transmission of epidemics. This network is composed of nodes, which correspond to individual agents, and links, which signify the connections between any two individuals. At its simplest, a contact network takes on a binary form with two distinct values:

a non-zero value denoting contact between a pair of individuals and 0 indicating no contact. Each node within this network represents an individual, while the interconnecting links between nodes provide insights into the quantity and types of interactions. For instance, these links shed light on an individual's associations with susceptible or infected individuals, thereby offering a comprehensive view of the underlying dynamics of disease transmission within the network.

In many cases, a single generic network is used to model epidemic diseases, but in reality, every network has some interaction with other networks. That's why the concept of interconnected networks is a very critical research area nowadays, especially for epidemic disease modeling [55, 56].

It is a proven result that in a generic contact network, if the ratio of infection to cure rate is less than a particular threshold, the infection cannot survive in the network. However, for SIS spreading dynamics in two interconnected networks, the epidemic can survive though the infection-to-cure rate in both networks is less than the epidemic threshold [57]. In that case, we have seen an epidemic threshold curve, which is plotted to show the epidemic threshold of one network as a function of effective infection strength (infection to cure rate) in the other network for a specific level of interconnection. To our best knowledge, this result has not been proven for SIR spreading dynamics.

In the initial portion of this chapter, we have demonstrated the alteration of the epidemic threshold of a specific network due to its coupling with another network, assuming a constant infection strength. However, we have specifically examined the change in the epidemic threshold concerning the dynamics of SIR spreading. We have plotted three distinct epidemic threshold curves correspond-

ing to three different types of coupling: weak, medium, and strong. We show that for SIR dynamics, although the epidemic threshold of both networks is less than the epidemic threshold, the infection can still survive in the whole interconnected system.

In our work in depicting the epidemic threshold curve for interconnected networks, the consideration has been that few initial infections either die out or invade both networks, causing an epidemic.

However, in reality, there are certain diseases where the infection is endemically present in one population represented by a contact network, and from that, the disease spills to another population represented by another contact network if the two networks are interconnected. This event is known as spillover.

In the second portion of this chapter, we have done significant work on spillover in various network-based models and obtained a clear phase transition for the probability of spillover. These network-based models for spillover include both homogeneous and heterogeneous node degree distributions. We have also drawn a spillover threshold curve based on inter-population link density and inter-network infection strength that divides the entire area into two regions: major and minor spillover. If the inter-network infection strength and interpopulation link density are in the major spillover region, the probability of spillover is very high, whereas if the inter-network infection strength and interpopulation link density are in the minor spillover region, the probability of spillover is low.

The rest of the chapter is organized as follows: Section 3.2 presents some background on spillover and interconnected networks. Section 3.3 illustrates the epidemic threshold curve for SIR dynamics in interconnected networks. Section

3.4 shows how to model spillover and discover the phase transition through extensive simulations.

3.2 Background

Multi-layer networks are formed by several networks that evolve and interact with each other. These networks are ubiquitous and include social networks, financial markets, and multi-modal transportation systems. The multi-layer structure of these networks strongly affects the properties of dynamical and stochastic processes defined on them, which can display unexpected characteristics [58].

As the field of network science has dramatically increased, researchers have found that most complex systems do not work in isolation. Every complex system depends on another complex system to some extent. For example, communication systems often depend on the power grid to be operational [59, 60]. So, if there is a failure in any part of an interconnected system, that fault propagates to other parts of the system. So, for the proper functioning of an interconnected system, insight into fault propagation mechanisms in an interconnected system is very important. This kind of research also provides insight into the robustness of the system [61]. Similarly, research has been done to revive a failed network through microscopic interventions. The complex system represented by a complex network generally fails due to node, link removal, or due to reduction in link weights. But just reversing the topological damage, i.e., reconstruction of links, nodes, or increase of link weight, does not guarantee the spontaneous recovery of a system. So scientists have come out with a two-step

intervention process by which a system can be steered towards its functionality after reversing the topological damage [62]. Radicchi et al. have shown that depending on the relative importance of inter and intra-layer connection, the entire interconnected system can have two regimes; in one regime, various layers act as independent entities, and in another regime, the whole system behaves as a single network [63]. These are some examples of various research conducted on interconnected networks.

Interconnected networks are also used to model epidemic spreading. Researchers have shown how the epidemic threshold of an interconnected network structure varies for SIS spreading dynamics without any approximation. They have also shown the upper and lower bound of the epidemic threshold and how it is related to properties of network parameters (eigenvalue and eigenvector) [64]. Scientists have found that for an interconnected network system, there exists a global threshold above which the infection prevails in every network of the subsystem and below which the infection dies out. Another finding indicated that having a diverse structure enhances the likelihood of infection, with this impact being particularly noticeable in interconnected network systems [65]. The epidemic threshold in two interconnected networks is always lower than any of the two-component networks. Moreover, in interconnected networks, interconnection correlation has no significant contribution to epidemic size [66]. Dickison and colleagues discovered that when considering SIR spreading dynamics within a connected network, there are two clear modes. In the case of strongly coupled interconnected networks, there's a threshold infection strength beyond which the epidemic invades the entire interconnected structure, while below this

threshold, the epidemics die away. But for weakly coupled networks, a mixed phase exists, where the epidemic does not spread in the whole interconnected system, and interconnections affect the less interconnected network mostly [67]. The directed interconnected network is also used for epidemic modeling. For various types of directed interconnected networks, mathematical expression of R_0. The disease will become endemic if R_0 is greater than 1; otherwise, it will die out. Coupling can increase R_0 and even make a disease endemic. There are certain considerations for epidemic prevalence in a single sub-network, which is only possible in directed network [68]. A new type of model has been made to investigate the epidemics on interconnected networks. One contact network has a fixed infection rate, and another has a periodic infection rate. They have some novel findings regarding R_0 based on their model and showed the dependence of infection rate and other network parameters on R_0 [69].

In recent years, many works have been done on modeling spillover. Nandi et al. have considered the effect of seasonal variation on transmission and recovery rates in the context of spillover. They have focused on the direct transmission of pathogens between humans and animals and considered all the infection and recovery rates are periodic. A branching process approximation has been applied near the disease-free equilibrium to predict the first spillover event. It also shows how the probability of spillover depends on the human-to-human infection rate, human-to-animal infection rate, and animal recovery rate [70]. Grange et al. have identified the host, viral, and environmental risk factors contributing to zoonotic virus spillover and spread in humans. They have also developed an interactive web tool that estimates the risk score of wildlife-origin viruses and

lists a number of viruses based on their risk score [71]. Ellwanger et al. have reviewed the basic aspects and the main factors involved in zoonotic spillover. The focus was on the role of inter-species interaction, phylogenetic distance between host and species, environmental drivers, and specific characteristics of the pathogen. They have also shed light on preventing zoonotic spillover in various ways [72]. Royce et al. have used a new mathematical spillover model with an intermediate host. The agents are in three categories: wild animals, domestic animals, and humans. They have assumed that the pathogen in domestic animals mutates itself and becomes strong enough to infect a human. Even though R_0 is less than 1 in humans, it can still infect the human population [73]. A synthetic framework for animal-to-human virus transmission is proposed by Plowright et al., and this study integrates the relevant spillover mechanism. According to the authors, all zoonotic pathogens must overcome a hierarchical series of barriers to cause spillover. If any barriers are impenetrable, then the spillover cannot happen. They describe these barriers in detail and claim that the probability of spillover is determined by the interaction among the barriers and the associated bottlenecks that might prevent cross-species transmission [74]. Rees et al. review the mathematical models of spillover. There are two criteria for selecting diseases included in models. The first one is the disease must be zoonotic, and the second one is the pathogen must be alive for 48 hours and should be able to infect humans. This appears to describe the scope of future research in zoonotic spillover, model validation, and other important information [75]. We have been discussing only zoonotic spillover till now, but recently, spillover from plants has also been spotted. A 61-year-old person

with no previous history of the disease has been infected by a plant fungus in Kolkata (a city in Eastern India). The scientific name of the plant pathogen is *Chondrostereum purpureum* [76].

3.3 Modeling SIR spreading in interconnected network

One of the most commonly employed compartmental models in epidemic modeling is the SIR model, which stands for Susceptible-Infected-Recovered. The SIR model is highly popular for understanding and predicting the spread of infectious diseases within a population.

S (Susceptible): A susceptible individual is someone who has the potential to become infected when exposed to an individual carrying the infection.

I (Infected): The infected individuals represent the people who have already contracted the disease and can transmit it to susceptible individuals.

R (Recovered): Recovered individuals are those who have previously been infected with the disease and have subsequently overcome it, resulting in immunity and no longer being capable of transmitting the infection.

The SIR model on a contact network with N number of agents is shown in Figure 3.1.

The equation of the SIR model with a mean-field approximation for i^{th} agent

in a network having N number of nodes (without considering demography) is

$$\frac{dS_i(t)}{dt} = -\beta \cdot S_i(t)(\sum_{j=1}^{N} a_{ij} I_j(t))$$
$$\frac{dI_i(t)}{dt} = \beta \cdot S_i(t)(\sum_{j=1}^{N} a_{ij} I_j(t)) - \delta \cdot I_i(t),$$
$$\frac{dR_i(t)}{dt} = \delta \cdot I_i(t).$$

Considering a node denoted by i within a network comprising N nodes, where each node is assigned labels ranging from 1 to N. The parameter β is the infection rate, and δ is the recovery rate. $S_i(t)$, $I_i(t)$, $R_i(t)$ denote the state probability of agent i being in the susceptible, infected, or recovered compartment, respectively. a_{ij} represents an entry in the network's adjacency matrix, where the values can only be 0 or 1. A nonzero value indicates a connection between agent i and agent j, while a value of 0 signifies the absence of a link between agent i and j. It can also be written that at any point in time, $S_i(t) + I_i(t) + R_i(t)$=1.

3.3.1 Generalized epidemic threshold curve

Let us consider two groups of agents of sizes: N_1 and N_2. Let's take the first graph, G_1, whose agents are labeled as 1 to N_1, and in the second graph, the agents are labeled as $(N_1 + 1)$ to $(N_1 + N_2)$. The adjacency matrix of graph G_1 is denoted by A_{11}, and the adjacency matrix of graph G_2 is denoted by A_{22}. The elements of sub-matrix A_{12} and A_{21} denotes the connection between node i and node j , where node i belongs to graph G_1 and node j belongs to graph

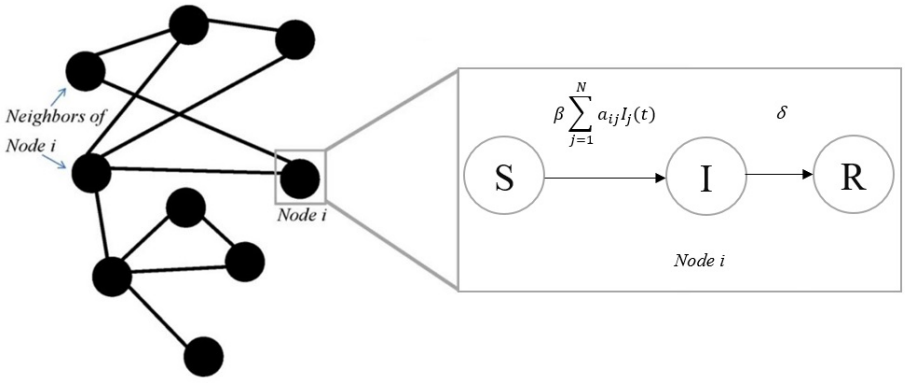

Figure 3.1: Schematic of a contact network along with the agent-level stochastic transition diagram for agent i according to the SIR epidemic spreading model. β and δ denote the infection and recovery rate, respectively. The notation a_{ij} is used to represent the connection between agent i and agent j. Specifically, if the value of a_{ij} is 0, it signifies the absence of a link between the two agents. Conversely, if a_{ij} is nonzero, it indicates the presence of a link between agent i and agent j. $I_j(t)$ is the state probability of being infected of node j at time t.

G_2. So, the adjacency matrix for the two interconnected networks is:

$$\begin{bmatrix} A_{11} & A_{12} \\ A_{21} & A_{22} \end{bmatrix}$$

The topology of networks G_1 and G_2 is undirected. As the interconnection between both networks G_1 and G_2 is undirected, it can be written as $A_{12} = (A_{21})^T$. The infection rates $\beta_{11}, \beta_{12}, \beta_{21}, \beta_{22}$ are such that a susceptible agent of graph G_m receives the infection from an infected agent of graph G_n with the infection rate, β_{mn} for $m, n \in [1, 2]$. The recovery rates of the agents of both networks are the same and equal to μ. The equations for the change in the state probability of infection of node i at time t for SIR spreading dynamics in the interconnected network can be expressed in the following manner:

$$\frac{dI_i(t)}{dt} = S_i(t) * [\beta_{11} \sum_{j=1}^{N_1} a_{ij} I_j(t) + \beta_{12} \sum_{j=N_1+1}^{N_1+N_2} a_{ij} I_j(t)] - \mu I_i(t); \;\; i = 1, .., N_1 \tag{3.1}$$

$$\frac{dI_i(t)}{dt} = S_i(t) * [\beta_{21} \sum_{j=1}^{N_1} a_{ij} I_j(t) + \beta_{22} \sum_{j=N_1+1}^{N_1+N_2} a_{ij} I_j(t)] - \mu I_i(t); \;\; i = N_1+1, .., N_1+N_2 \tag{3.2}$$

Our assumption is that if there is no interconnection, then infection cannot survive in G_2; that is, β_{22}/μ will be less than the epidemic threshold of G_2. So, in our case, the effective infection strength β_{22}/μ will be between zero to $1/\lambda(A_{22})$. Here $\lambda(A_{22})$ is the highest eigenvalue of A_{22}.

As the initial fraction of infected individuals is very small, we can assume that $S_i(0) \approx 1$. So, equations (1) and (2) can be written as follows:

$$\frac{dI_i(t)}{dt} \approx [\beta_{11} \sum_{j=1}^{N_1} a_{ij} I_j(t) + \beta_{12} \sum_{j=N_1+1}^{N_1+N_2} a_{ij} I_j(t)] - \mu I_i(t); \;\; i = 1, .., N_1 \tag{3.3}$$

$$\frac{dI_i(t)}{dt} \approx [\beta_{21} \sum_{j=1}^{N_1} a_{ij} I_j(t) + \beta_{22} \sum_{j=N_1+1}^{N_1+N_2} a_{ij} I_j(t)] - \mu I_i(t); \;\; i = N_1+1, .., N_1+N_2 \tag{3.4}$$

To find the epidemic threshold, we follow the approach of Youssef et al. [77].

Equations (3) and (4) can be written as follows:

$$\frac{dI_i(t)}{dt} \approx \sum_j L_{ij} I_j(t). \tag{3.5}$$

The element $L_{ij} = (\beta a_{ij} - \mu \delta_{ij})$ of equation (5) is the element of the Jacobian matrix L defined as follows (equation (6)).

$$L = \begin{bmatrix} \beta_{11}A_{11} & \beta_{12}A_{12} \\ \beta_{21}A_{21} & \beta_{22}A_{22} \end{bmatrix} - \mu * I_{(N1+N2)(N1+N2)} \tag{3.6}$$

where δ_{ij} is the Kronecker delta function and $I_{(N1+N2)(N1+N2)}$ is the identity matrix of dimension $(N1+N2)(N1+N2)$. We now perform the spectral analysis of the Jacobian matrix to study the growth or decay of epidemics in interconnected systems. In the above-mentioned Jacobian matrix, the elements were in the form of $\beta a_{ij} - \mu\delta_{ij}$. However, instead of using these elements in the form of $\beta a_{ij} - \mu\delta_{ij}$, we can write them as $\mu[\tau a_{ij} - \delta_{ij}]$, where $\tau = \beta/\mu$. Now a new matrix $\bar{L}$ can be constructed where each element will be in the form $[\tau a_{ij} - \delta_{ij}]$.

For interconnected graphs, this new matrix $(\bar{L})$ is shown in equation (7)

$$\bar{L} = \begin{bmatrix} \tau_{11}A_{11} & \tau_{12}A_{12} \\ \tau_{21}A_{21} & \tau_{22}A_{22} \end{bmatrix} - I_{(N1+N2)(N1+N2)} \tag{3.7}$$

where $\tau_{11} = (\beta_{11}/\mu); \tau_{12} = (\beta_{12}/\mu); \tau_{21} = (\beta_{21}/\mu); \tau_{22} = (\beta_{22}/\mu)$. Thus, we can define $L = \mu\bar{L}$. Let us denote the matrix $\bar{L}$ as $[\widetilde{L} - I]$. It is known that a system with negative eigenvalues indicates that perturbations will decay over time, leading the system towards stability. Since the recovery rate, μ, is a positive quantity, it follows that if the eigenvalues of $[\widetilde{L} - I]$ are all less than zero, the disease will not spread throughout the entire network system. This insight is crucial for understanding the stability and containment of epidemic spread in network structures. To ensure the epidemic threshold condition is met, the maximum eigenvalue of $\widetilde{L}$ must be 1. Given that the overall network is connected, $\widetilde{L}$ is an irreducible, non-negative square matrix. The largest absolute

value of any eigenvalue of a matrix is called its spectral radius. According to the Perron-Frobenius theorem [78], for an irreducible, non-negative square matrix $\widetilde{L}$, the spectral radius is a real, positive, and simple eigenvalue. Furthermore, the corresponding Perron vector is strictly positive. Let V_1 and V_2 denote the Perron vectors when the spectral radius equals 1.

So, for a spectral radius equal to 1, we can write as follows:

$$\begin{bmatrix} \tau_{11}A_{11} & \tau_{12}A_{12} \\ \tau_{21}A_{21} & \tau_{22}A_{22} \end{bmatrix} \begin{bmatrix} V_1 \\ V_2 \end{bmatrix} = \begin{bmatrix} V_1 \\ V_2 \end{bmatrix} \tag{3.8}$$

Based on equation no. (8) above, we can write the equations below (9 and 10).

$$\tau_{11}A_{11}V_1 + \tau_{12}A_{12}V_2 = V_1 \tag{3.9}$$

$$\tau_{21}A_{21}V_1 + \tau_{22}A_{22}V_2 = V_2 \tag{3.10}$$

Finding the value of V_2 from equation (10), we get

$$V_2 = \tau_{21}(I - \tau_{22}A_{22})^{-1}A_{21}V_1 \tag{3.11}$$

As V_1 is positive, it follows that $V_2 = \tau_{21}(I - \tau_{22}A_{22})^{-1}A_{21}V_1$ exists and is non-negative. By substituting the expression for V_2 into equation (11) and then into equation (9), we can rewrite equation (9) as $HV_1 = V_1$, where H is given by:

$$H = \tau_{11}A_{11} + \tau_{21}\tau_{12}A_{12}(I - \tau_{22}A_{22})^{-1}A_{21}. \tag{3.12}$$

We know that the infection process is the result of interactions between pairs of agents. It depends on the rate at which the disease is transmitted and the ability

of the susceptible to receive the disease. So $\beta_{11}, \beta_{12}, \beta_{21}, \beta_{22}$ are not completely independent on each other. Following the analysis of the infection rates in any interconnected network [57], we can write.

$$\beta_{12}\beta_{21} = \alpha^2\beta_{11}\beta_{22} \tag{3.13}$$

As the recovery rates for all the agents are same, we can write the equation (13) as

$$\tau_{12}\tau_{21} = \alpha^2\tau_{11}\tau_{22} \tag{3.14}$$

Here α is a positive scalar accounting for the heterogeneity of interconnection and intraconnection. So, by substituting equation (14) in equation (12), we obtain

$$H = \tau_{11}A_{11} + \alpha^2\tau_{22}\tau_{11}A_{12}(I - \tau_{22}A_{22})^{-1}A_{21}. \tag{3.15}$$

We can update equation (15) as $H = \tau_{11}H_T$, where H_T can be defined as

$$H_T = [A_{11} + \alpha^2\tau_{22}A_{12}(I - \tau_{22}A_{22})^{-1}A_{12}^T] \tag{3.16}$$

As we have stated, equation (9) can be expressed in the form of $HV_1 = V_1$, so from equations (15) and (16), we can also update the expression $HV_1 = V_1$ as

$$\tau_{11}H_TV_1 = V_1 \tag{3.17}$$

We said V_1 is a Perron vector, which is positive, and from the analysis of Sahneh et al. [57], we can conclude that H_T is an irreducible matrix. Therefore,

from the Perron-Frobenius Theorem for irreducible matrices, we can conclude that τ_{11} is the inverse of the spectral radius of H_T.

If we call the epidemic threshold τ_{11c}, we can say that τ_{11c} is the spectral radius of the matrix H_T, which is denoted in equation (16). So, for any given infection strength τ_{22} and coupling level, if the τ_{11} value is lower than τ_{11c}, we can say the epidemic will die out.

3.3.2 The threshold curve

To give an example of application of the results obtained in the previous section, we have generated two different realizations of the Watts-Strogatz (WS) model [79]. In layer 1, we have a WS network with 500 nodes, a mean node degree of 20, and a rewiring probability of 0.2. In layer 2, we have a WS network with 100 nodes, a mean degree of 4, and a rewiring probability of 0.1. We have activated all potential edges between the two layers with some probability ω for the interconnection of these two graphs. For high, medium, and low interconnection levels, the values of ω are respectively 0.2, 0.042, and 0.01. We have generated a plot of the normalized epidemic threshold $\tau_{c1} = \tau_{11,c}\lambda(A_{11})$ as a function of the normalized infection strength $\tau_2 = \tau_{22}\lambda(A_{22})$ for different interconnection levels. The plot of epidemic threshold curves is shown in Figure 3.2.

We have taken various normalized epidemic strengths (τ_{c1} and τ_2) and found that when the epidemic strengths are below the threshold curve, the infection is not spreading, whereas when the infection strengths are above the threshold curve, the infection is spreading. This is true for any level of interconnection.

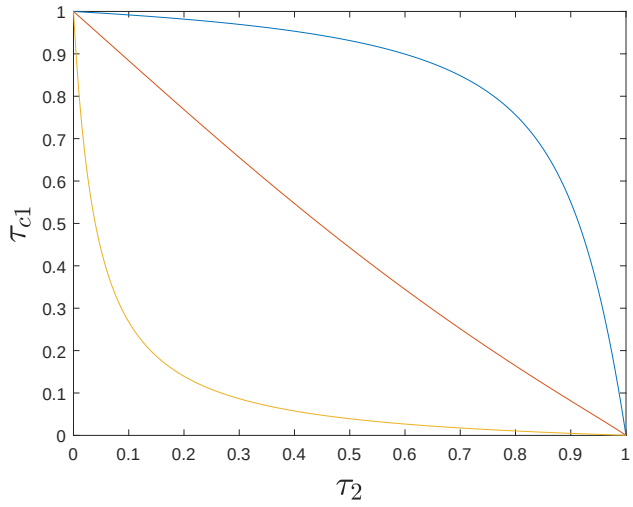

Figure 3.2: Graph of normalized epidemic threshold τ_{c1}=$\tau_{11,c}$*$\lambda(A_{11})$ as a function of normalized infection strength τ_2=τ_{22}*$\lambda(A_{22})$ with different interconnection levels and α=1. The yellow curve is for a strong level of interconnection (ω=0.2), the red curve is for a medium level of interconnection (ω=0.042), and the blue curve is for a low level of interconnection (ω=0.01). The curve shown in this figure is for the above-mentioned small-world network topology.

Through the following figures, we have shown how the number of agents in different compartments varies with time. The network topologies are the same Watts-Strogatz models as mentioned earlier. In the given scenario where the normalized infection strengths (τ_{c1} and τ_2) for both network one and network 2 are 0.4, and the inter-network infection strengths are equal with a value of alpha being 1, as well as a recovery rate of 1 for the agents of both networks, we observe that the epidemic is spreading when the level of interconnection between the networks are strong (Figure 3.3). Conversely, when the level of interconnection is weak, the epidemic does not spread (Figure 3.3).

We have also plotted the epidemic threshold curves for the Erdos-Renyi network. [80] (Figure 3.4). The first layer is a Gilbert model with 500 nodes and a probability of interconnection of 0.02. The second layer is a Gilbert model with 100 nodes and a probability of interconnection of 0.1. For this configuration, the epidemic threshold curve is shown in Figure 3.4

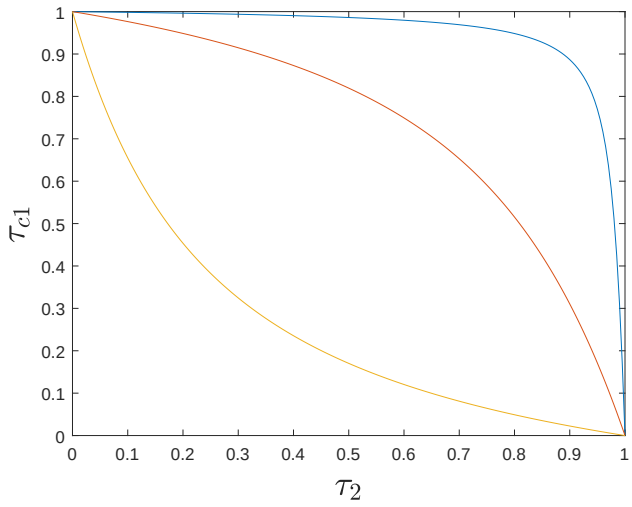

Figure 3.4: Graph of normalized epidemic threshold τ_{c1}=$\tau_{11,c}$*λ(A11) as a function of normalized infection strength τ_2=τ_{22}*λ(A22) with different interconnection level and α=1 for Gilbert networks. The yellow curve is for the high number of interconnections (ω=0.2), the red curve is for a medium number of interconnections (ω=0.042), and the blue curve is for a low number of interconnections (ω=0.01). The network topologies for both networks are Erdos-Renyi.

We have also plotted the epidemic threshold curve for an interconnected network system where both the network is an Erdos-Reyni network of 500 nodes, and the probability of interconnection is 0.02. The curve is shown in Figure 3.5

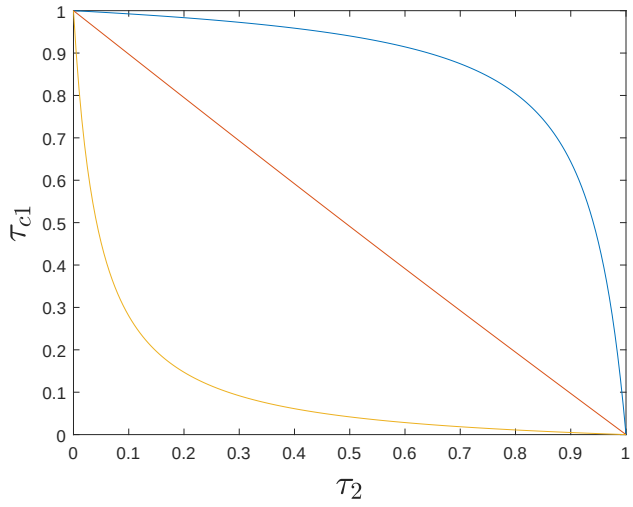

Figure 3.5: Graph of normalized epidemic threshold τ_{c1}=$\tau_{11,c}$*λ(A11) as a function of normalized infection strength τ_2=τ_{22}*λ(A22) with different interconnection level and α=1 for Gilbert networks. The yellow curve is for the high number of interconnections (ω=0.2), the red curve is for a medium number of interconnections (ω=0.042), and the blue curve is for a low number of interconnections (ω=0.01). The network topologies for both networks are Erdos-Renyi.

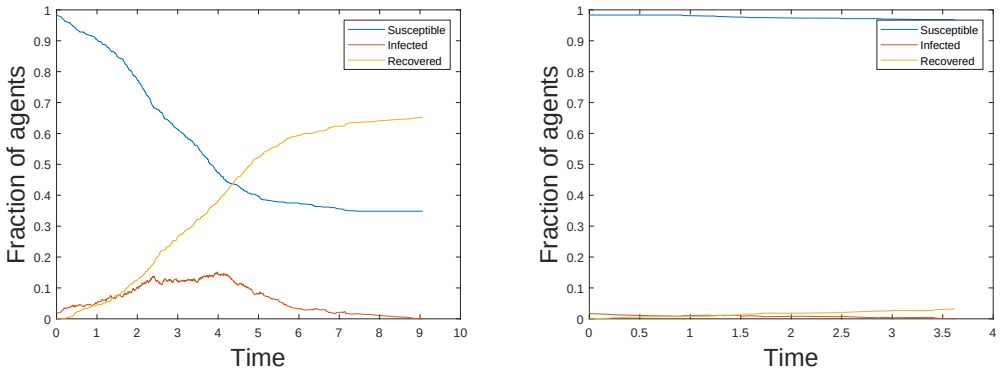

Figure 3.3: Figures depicting spreading scenarios for weak and strong-level interconnections. The figure shows that when the normalized epidemic strengths are above the threshold, the infection spreads in the contact network (left). When the normalized epidemic strengths are below the threshold, the infection spreads in the contact network (right).

3.4 Modelling Spillover

Spillover refers to transferring a virus from its usual circulating species, known as the reservoir, to a different species, known as the novel host. In the host species, the virus can either perish or undergo adaptations, potentially leading to the emergence of an epidemic. Zoonotic infectious diseases spread from animals to humans. Sixty percent of human infectious diseases are zoonotic, and seventy-five percent are emerging zoonoses [81]. Many emerging zoonotic diseases are caused by viruses, including avian influenza, rabies, and Ebola[82, 70].

The graphical representation in Figure 3.6 illustrates the transfer of infection, referred to as spillover. The upper network represents a reservoir network, where the nodes are highlighted in red. The lower network represents the population of a novel host, with its nodes marked in blue. The red and blue links between the agents of reservoir and novel host population network denotes the intra network connection between the agents. The black-directed links indicate the transmission of the disease from the infected agents in the reservoir network to the agents in the novel host population network.

In a contact network where there are already some infected individuals, the spread of a disease can occur, and various factors influence the extent of the spread. However, if we keep all other properties of the network constant, it has been observed that when the initial number of infected individuals is low, the threshold for an epidemic to occur becomes higher. This means that if the initial number of infected individuals is very low, the spread of the disease can be controlled [83].

In our work, when the number of infected individuals in the new host net-

work exceeds a significant threshold (considered as three), it indicates an effective spillover event. Therefore, if the number of infected agents resulting from spillover in the host network is less than three, the spillover size is considered zero. Similarly, if the probability of spillover in the host network (calculated as the ratio of spillover occurrences to the total number of realizations) is less than 0.1, it is classified as a non-spillover scenario. These assumptions are in line with previous research on the stochastic epidemic model [84].

To simulate the spillover events, we have used the stochastic simulator GEMFsim based on the Generalized Epidemic Mean Field (GEMF) framework developed by the Network Science and Engineering (NetSE) group at Kansas State University [49, 50]. We have used the Matlab and Python version for simulation.

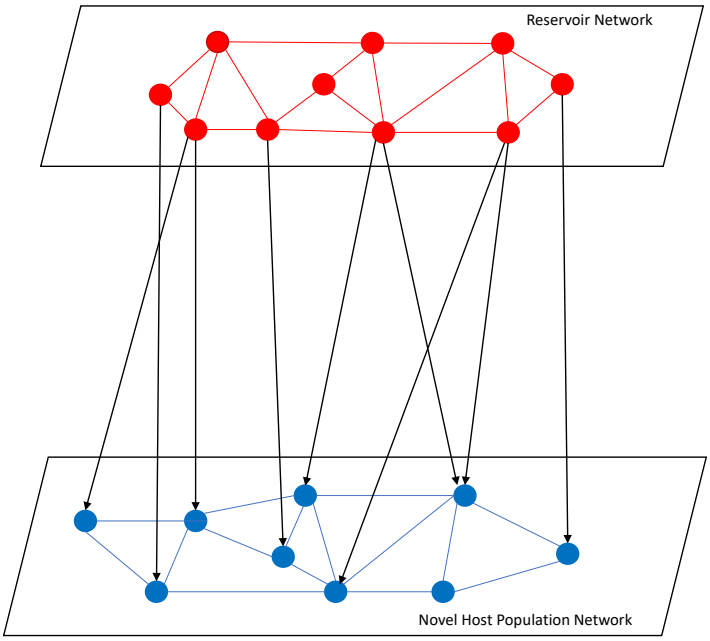

Figure 3.6: Spillover in networks from reservoir population to the novel host population.

3.4.1 Simulation results

Our simulation model pertains to diseases like avian influenza, West Nile virus, and Ebola. In the first portion of our simulation based study we have modeled avian influenza and West Nile virus diseases.Transmission of avian influenza occurs primarily from birds to other birds and occasionally from birds to humans. For West Nile disease, the mechanism of transmission is different. The disease mainly circulates between mosquitoes and birds, which can infect each other and be infectious. When mosquitoes cannot find birds, they sometimes target mammals and can infect them (such as humans). Mammals cannot transmit the disease and are known as dead-end hosts. Hosseini et al. have explained

the mechanism of West Nile virus transmission using a system of differential equations and employ this model to predict the number of new cases [85]. Our network-based model for West Nile disease and avian influenza in this simulation study draws inspiration from the work of Moon et al. [51]. In our simulation-based study of avian influenza and West Nile virus, we can envision a scenario in which the agents within the reservoir network represent birds while the agents in the novel host population network represent humans. Consequently, within our spillover model, we establish an effective infection rate of zero between the agents in the novel host population network. Conversely, both the effective infection rate within the reservoir network and the effective infection rate between the novel host population network and the reservoir network are non-zero.

The examination of data from the 2019 European study [86] revealed that the percentage of infected birds can vary significantly due to various factors. With this study as a reference, we aim to establish an effective infection rate within our reservoir network such that the number of infected agents in the reservoir network falls within the range of 4 to 6 percent of the total population. Notably, the study [86] found that, on average, 5.6 percent of birds were infected with Highly Pathogenic Avian Influenza (HPAI) in eight European countries.

In this specific situation, both the novel host network and reservoir network are Erdos-Renyi networks consisting of 1000 nodes and 3255 links. Throughout the simulation, the infection rates have been set as follows. The infection rate within reservoir network β_{22} is set to 0.15 in order to obtain the expected number of infected agents to be within 4 to 6 percent of the total population as reported in [86].

Now, the probability that a human is infected by a bird can vary a lot based on different factors like virus strain, immunity of people, infection-spreading capability of birds, etc. However, based on a study conducted on Egyptian people, the probability of a person being infected by a poultry bird is 0.02 [87]. Another study conducted in European countries claims that the risk of avian influenza for general people is low, and for occupationally exposed people, the risk of infection is low to medium [88]. Based on these studies, the infection rate between agents of the reservoir network and the novel host population network β_{12} is set equal to 0.02 such that the probability of infection for humans from birds is 0.02, and the rate is also low to moderate. Finally, we set the infection rate within the novel host population network β_{11} equal to 0, assuming human-to-human disease transmission is very limited. The recovery rate δ for all agents is assumed to be equal to 1 to maintain a proper effective infection rate. The fraction of the total number of interpopulation links between the two networks has ranged from 0.0001 to 0.03. To establish an interpopulation link, we randomly select one node from the reservoir network and one node from the novel host population network, creating a directed link from the reservoir network to the novel host population network.

To measure the spillover size, 16000 simulations have been conducted for each fraction of all possible links. For each specific fraction of links, a box plot has been generated to depict the spillover size (Figure 3.7). Ten random nodes were chosen as initially infected nodes in the reservoir network. This random selection process was repeated for each realization, resulting in different sets of initially infected nodes for each iteration.

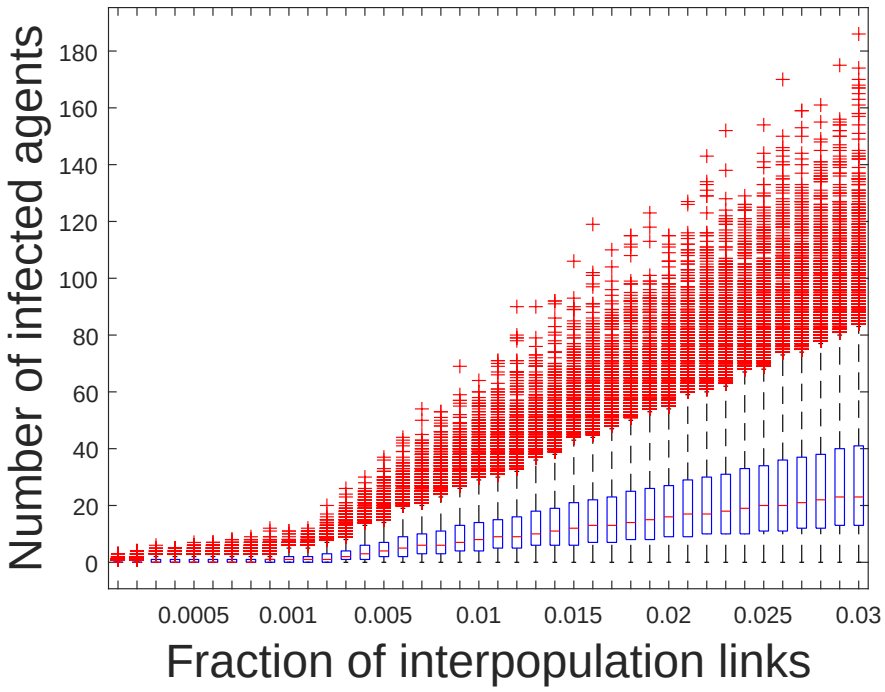

Figure 3.7: The number of infected agents in novel host population network due to spillover with the fraction of total possible links between novel host population network and reservoir network. Every 16000 realizations have been shown in the boxplot.

Based on the assumptions about spillover mentioned earlier in this paper, we have generated a plot between the probability of spillover in the host network and the fraction of links between the reservoir and the host network (Figure 3.8).

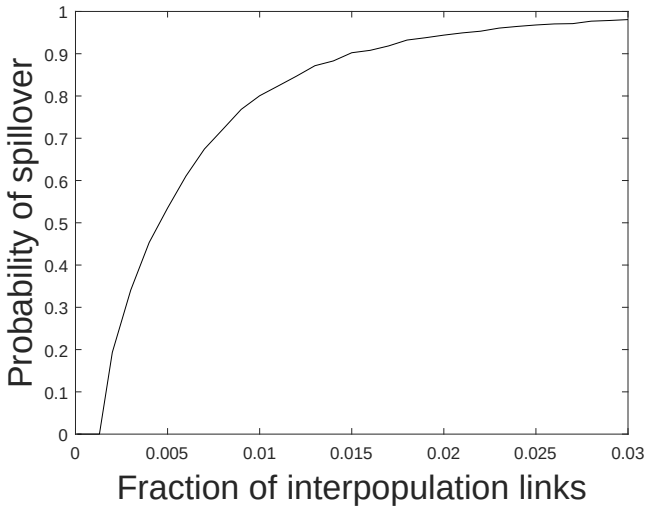

Figure 3.8: Probability of spillover in novel host population network with inter-population link density. All other parameters are kept constant.

It is important to mention that when the fraction of links is smaller than 0.0013, the probability of spillover remains very low. However, beyond this threshold, there is a noticeable increase in the probability of spillover. Therefore, we can conclude that the fraction of 0.0013 of the total possible inter-network links acts as a clear threshold, indicating a distinct phase transition.

In the next scenario, the number of links between the novel host population network and reservoir network has been kept constant at 1000. However, the inter-network infection rate (β_{12}) has been systematically reduced from 0.7 to 0.005. The infection rate within the novel host population network (β_{11}) is set to zero, while the infection rate within the reservoir network (β_{22}) remains at 0.15. The novel host network and the reservoir network maintain the same topology as previously mentioned. It is assumed that ten random nodes are

infected during each iteration.

To analyze the impact of different inter-network infection rates on spillover size, 16000 realizations have been recorded for each value of inter-network infection rate. For each inter-network infection strength, a box plot has been generated to represent the spillover size visually (Figure 3.9).

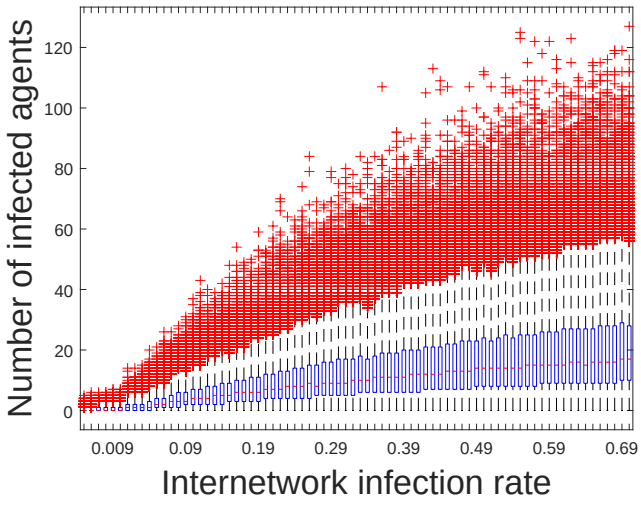

Figure 3.9: The number of infected agents in novel host population network with the inter-network infection rate between novel host population network and reservoir network. Every 16000 realizations have been shown in the boxplot. These boxplots are generated in Matlab

Based on the previously mentioned assumptions about spillover, we draw a curve between the probability of spillover and inter-network infection strength between two networks (Figure 3.10).

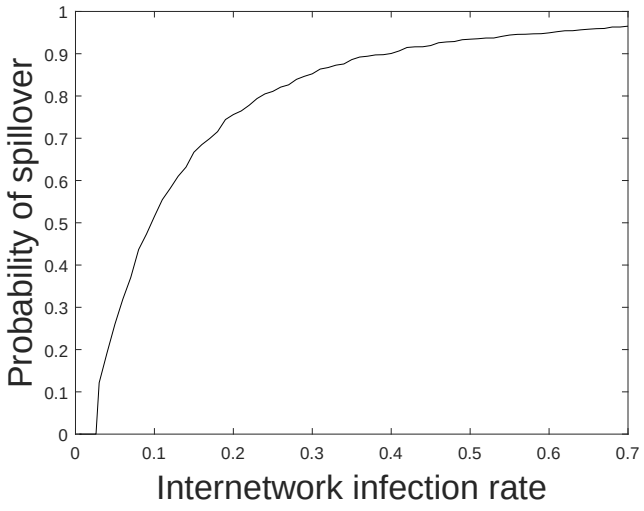

Figure 3.10: Probability of spillover with inter-network infection rate keeping all other parameters constant.

If we observe Figure 3.10 closely, we can see that the inter-network infection rate close to 0.026 acts as a threshold between a low and significantly high probability of spillover. A clear phase transition in spillover probability also exists for the change in inter-network infection rate.

When all other factors remain unchanged, and the fraction of total possible links between different populations exceeds approximately 0.001 in a fixed network structure, we can observe a relationship between the strength of infection between networks (β_{12}) and the total fraction of inter-population links between populations. This relationship confirms the validity of our assumption regarding the extent of spillover events. In fact, the strength of infection between networks (β_{12}) and the proportion of links between populations are inversely proportional to each other. Based on this correlation, we can represent a rect-

angular hyperbola curve where either of these two quantities can be plotted on the x-axis and the other on the y-axis (Figure 3.11). The region above this curve (shown in green in Figure 3.11) corresponds to a significant spillover area, while the region below the curve represents a minor spillover area (shown in yellow in Figure 3.11).

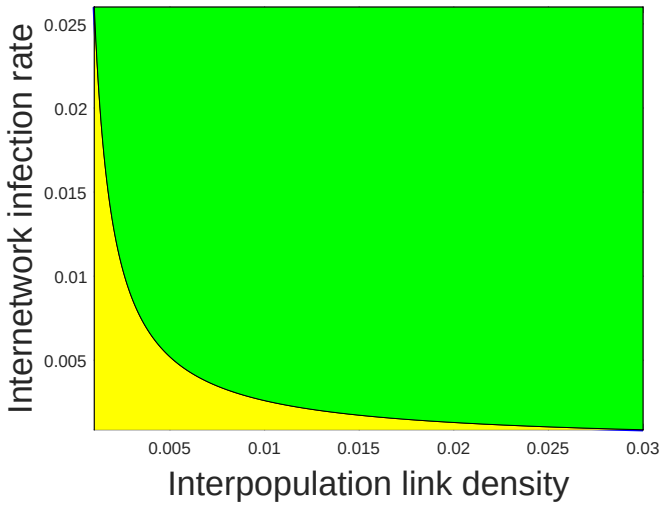

Figure 3.11: Spillover region separation based on inter-population links and inter-network infection strength. The green-colored zone is the significant spillover zone, while the yellow zone is the non-significant spillover zone.

Furthermore, we conducted the same experiment with scale-free networks [89] in both layers. There were no significant changes in the results compared to the previous findings when the inter-network links between the host and reservoir networks were randomly connected.

However, when the agents of the novel host network were connected with the hubs of the reservoir network using the same inter-network infection rate, a

phase transition occurred at a significantly lower fraction of links compared to the previous results shown in Figure 3.8. In this case, we had a scale-free network consisting of 1000 nodes and 2957 links for both the novel host population network and the reservoir network. The infection rate among the agents of the reservoir network was 0.1, and the inter-network infection rate was 0.02. We distributed the number of links equally among five hubs. However, the fraction of links varied from 0.0001 to 0.0039, and for each fraction of links, we conducted 16000 realizations to illustrate the size of spillover, shown in the boxplot (Figure 3.12). We observed the same phase transition in the spillover probability as before, but it occurred when the fraction of inter-population links was much smaller, approximately 0.00018 (Figure 3.13).

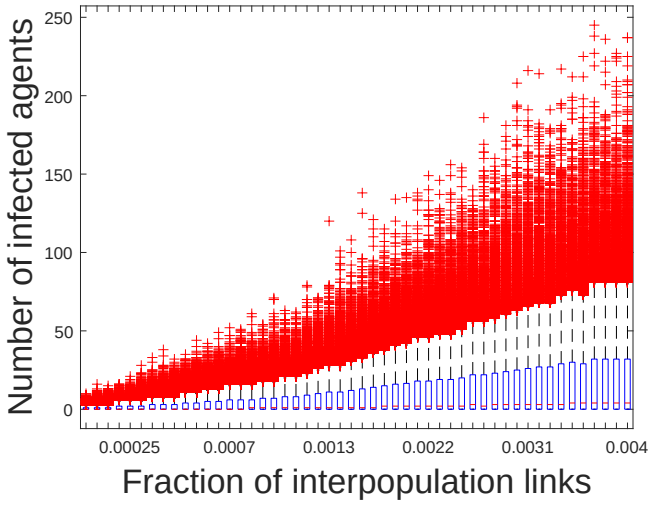

Figure 3.12: The inter-population links are connected with only the hubs of the reservoir network. The spillover size for each fraction of links has been shown in boxplot

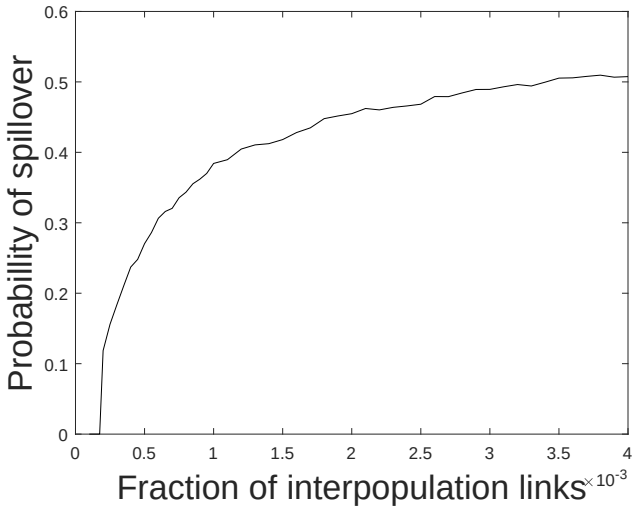

Figure 3.13: The phase transition curve when the inter-population links between novel host population network and reservoir network are connected with the hubs of reservoir network. The phase transition occurs for a very low fraction of links.

In our study, we expanded our simulations to include small-world networks (based on Watts and Strogatz's model) and observed that the same phase transition phenomenon also exists for these networks.

To summarize, the primary focus of our simulations was on exploring the spillover threshold. To achieve this, we selected random networks, scale-free networks, and several small-world networks with varying rewiring probabilities (ranging from 0.01 to 1). All of these networks contained the same number of nodes (1000), while the small-world networks had a slightly higher number of links.

During the course of the experiments, we carefully controlled the infection rate to ensure that the average number of total infected individuals within the

reservoir network remained consistently stable. Across all mentioned network topologies, this average ranged around 5 percent throughout the entire infection process. Additionally, the inter-network infection strength (β_{12}) was kept constant. Our goal was to measure the number of inter-population links required to reach the spillover threshold. For this threshold, we validated our previous assumption, stating that approximately 0.1 fractions of all realizations would exhibit a spillover non-negligible spillover size.

Our findings revealed that the number of links needed to reach the spillover threshold was the lowest for scale-free networks and the highest for regular lattice networks. As for the small-world networks, an increase in the rewiring probability resulted in a decrease in the number of inter-population links required to reach the spillover threshold. This behavior can be attributed to the emergence of the small-world effect, which promotes the spread of epidemics [90].

In the case of scale-free networks, the presence of hubs, which are highly connected nodes, contributed to an enhanced spread of epidemics within the network.

In another scenario, our simulation-based study has been expanded to discuss one of the most notorious zoonotic diseases, Ebola, which is prevalent in West African countries. Unlike other infections where humans serve as dead-end hosts, Ebola can also spread through human networks. The Susceptible-Exposed-Infected-Recovered (SEIR) model is particularly apt for modeling Ebola due to its ability to incorporate the incubation period before the disease becomes transmissible. This model enhances the SIR model by introducing an 'Exposed'

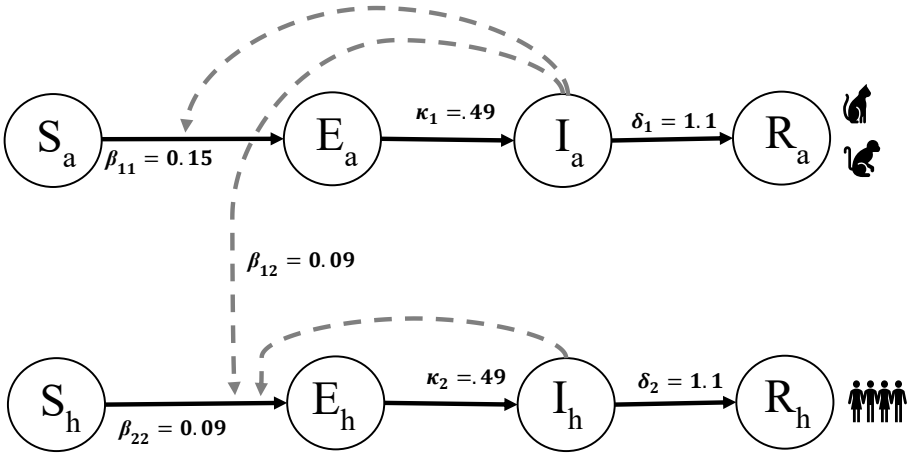

Figure 3.14: SEIR Transition Graph for Ebola Across Interconnected Networks. The diagram illustrates the transition rates between SEIR states, a and h subscript denote to animal and human agents, respectively. Parameters β_{11} and β_{22} represent the infection rates between the agents of the novel host population network and reservoir network, respectively. and β_{12} denotes infection rate between the agents of the reservoir network and novel host population network ; κ_1 and κ_2 indicate the incubation rates of animals and humans respectively that lead to infectious states; δ_1 and δ_2 are the recovery rates of animals and humans respectively. Dashed arrows show the inducing state for transitions.

state that accounts for the incubation period. The transition between states in the SEIR model, as shown in 3.14, includes the incubation rate (κ), which is incubation rate related the time it takes for an exposed individual to become infectious.

In this analysis, we examine a hypothetical yet plausible scenario for the transmission of the Ebola virus from animal reservoirs to human populations. To enhance the realism of our model, we constructed two distinct network layers. The first layer, representing the animal population, is modeled as a stochastic block network comprising 2000 nodes and 5079 undirected edges. This network simulates 20 distinct animal herds, where each block represents a particular herd, each connected to at least two other herds, mimicking the potential inter-

herd transmission dynamics. For the human population layer, we employed a Barabási-Albert (BA) network to represent a small village setting. The BA network, renowned for its scale-free properties, accurately captures the intricate social structures present in human communities, featuring 5000 nodes and 14991 undirected edges. In Figure 3.15, an example of these two networks structure is presented. We extracted the parameters for the SEIR model from the cases covered in [91] as Uganda 2000 case and adjusted the rates to accurately reflect the network structure for both humans and animals. The rates were adapted based on the average degree of nodes $\langle k \rangle$. The parameters used for this experiment are detailed in Figure 3.14.

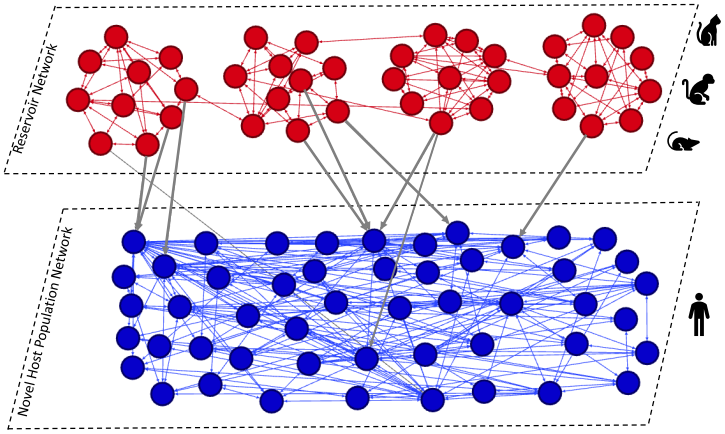

Figure 3.15: Illustration of an example for two-layer network structure used in the simulation: (a) represents the contact network among animals, (b) represents the contact network among humans, and the grey arrows denote the directed transmission links from animals to humans.

We ran 16000 simulations to examine the effects of varying the number of links between humans as hosts and animals as networks as we increase the links from 100 to 30,000 edges. Figure 3.16 shows the number of infected agents in the novel host population network for a specific fraction of interpopulation links. The data from a total of 16,000 simulation realizations is represented using a boxplot. The probability of spill-over with respect to the fraction of interpopulation links is also presented in Figure 3.17. In this simulation-based study, we can also see a clear phase transition for the probability of spillover as the number of interpopulation links increases. A fraction of up to 0.0001 of the total possible number of links acts as a threshold for this phase transition curve.

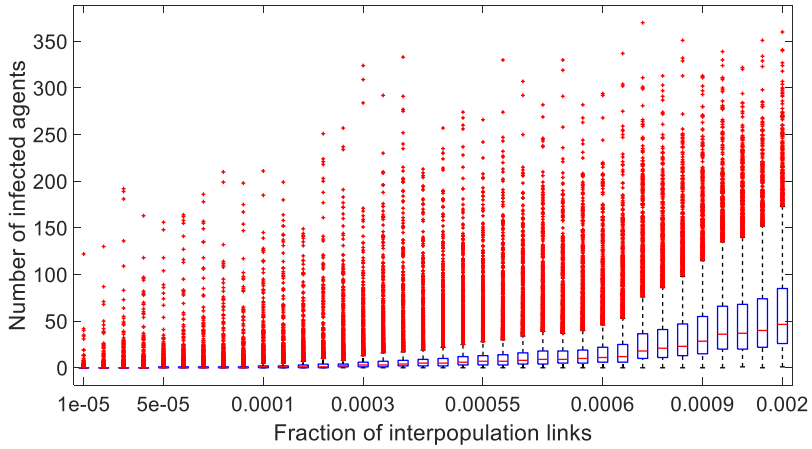

Figure 3.16: The boxplot of number of infected agents in novel host population network for the simulation-based study of Ebola. The number of infected agents in the novel host population network increases with the fraction of the possible links between the novel host population network and the reservoir network.

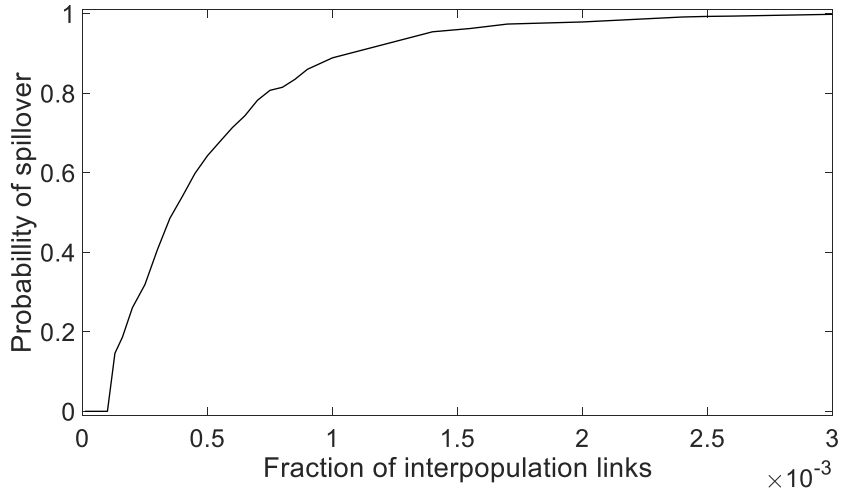

Figure 3.17: Probability of spillover in host population network for simulation-based study of Ebola

Based on the simulation-based study of the above-mentioned zoonotic diseases, we can conclude that there will always be a clear phase transition in the probability of spillover as the number of interpopulation links increases, regardless of whether humans act as dead-end hosts.

Chapter 4

Conclusions

My thesis investigated two scenarios for SIR spreading dynamics in interconnected networks. In the first case, we have a situation where the initial infection could be present in any of the two interconnected networks. The infection will not spread in interconnected networks if the normalized infection strengths are below the threshold curve for any level of interconnection. However, in the second situation, the infection in the novel host population comes only from the reservoir network. For avian influenza and West Nile virus modeling, we conducted experiments by changing the number of inter-population links and by changing the inter-network infection rate, keeping all other parameters constant. Experiments have been conducted on Erdos-Renyi networks, Barabasi-Albert networks, and Watts-Strogatz networks. The inter-population links were distributed randomly. In all the cases, we obtained a phase transition in the probability of spillover. While keeping all other network parameters constant, we obtain a relationship between the inter-population link density and inter-

network infection strength, based on which we get two regimes of significant and minor spillover zones. When the inter-population links are connected only with the hubs, we get a phase transition at a very low number of links while keeping all other parameters constant. It can be concluded that hubs of scale-free networks also play a crucial role in spillover. For small-world networks, we found that the number of interpopulation links for the spillover threshold decreases with the increase in rewiring probability. The spillover threshold, when considering a fixed number of infections in the reservoir population, follows a pattern of highest to lowest interpopulation links: Regular Lattice networks have the highest number of links, followed by Small-World networks, Erdos-Renyi networks, and finally Scale-Free networks with the lowest number of links. Finally, when we expanded our simulation-based study to model Ebola, where human-to-human infection spreading is significant, we observed a clear phase transition in the probability of spillover.

For future work, this study can be enhanced by developing a theoretical model to determine the spillover threshold for both inter-population links and inter-network infection strength. Additionally, simulations using various network topologies and inter-population link patterns can provide diverse results. These simulation outcomes can be used to train a neural network for predicting spillover in new scenarios.

4.1 Abbreviations

- ENM: Ecological Niche Modeling
- SIR: Susceptible-Infected-Recovered
- SIS: Susceptible-Infected-Susceptible
- SEIR: Susceptible-Exposed-Infected-Recovered
- SEIV: Susceptible-Exposed-Infected-Vaccinated
- AHSv: African Horse Sickness viruses
- WS: Watts-Strogatz
- GEMF: Generalized Epidemic Mean Field
- NetSE: Network Science and Engineering
- HPAI: Highly Pathogenic Avian Influenza
- BA: Barabási-Albert
- MaxEnt: Maximum Entropy
- GARP: Genetic Algorithm for Rule-set Prediction
- AUC: Area Under Curve
- ROC: Receiver Operating Characteristics
- JEV: Japanese encephalitis virus
- WNV: West Nile virus

- RVFV: Rift Valley fever virus
- COVID-19: Coronavirus disease 19
- SEIATR: Susceptible-Exposed-Infected-Asymptomatic-Treatment-Recovered

Bibliography

[1] S. Das, M. H. Samaei, and C. Scoglio, "SIR Epidemics in Interconnected Networks: threshold curve and phase transition," *Applied Network Science*, 2024.

[2] A. Aschengrau and G. R. Seage, *Essentials of epidemiology in public health*. Jones & Bartlett Publishers, 2013.

[3] D. E. Lilienfeld, "Definitions of epidemiology," *American journal of epidemiology*, vol. 107, no. 2, pp. 87–90, 1978.

[4] A. S. Evans, "Re:"Definitions of epidemiology"," *American Journal of Epidemiology*, vol. 109, no. 3, pp. 379–382, 1979.

[5] M. Frérot, A. Lefebvre, S. Aho, P. Callier, K. Astruc, and L. S. Aho Glélé, "What is epidemiology? Changing definitions of epidemiology 1978-2017," *PloS one*, vol. 13, no. 12, p. e0208442, 2018.

[6] M. Marathe and A. K. S. Vullikanti, "Computational epidemiology," *Communications of the ACM*, vol. 56, no. 7, pp. 88–96, 2013.

[7] J. Graunt and W. F. Willcox, "Natural and political observations made upon the bills of mortality," *(No Title)*, 1939.

[8] D. Bernoulli, "Réflexions sur les avantages de l'inoculation," *Mém. Paris*, vol. 1, pp. 439–482, 1758.

[9] D. Bernoulli and D. Chapelle, "Essai d'une nouvelle analyse de la mortalité causée par la petite vérole, et des avantages de l'inoculation pour la prévenir," 2023.

[10] D. Bernoulli and S. Blower, "An attempt at a new analysis of the mortality caused by smallpox and of the advantages of inoculation to prevent it," *Reviews in medical virology*, vol. 14, no. 5, p. 275, 2004.

[11] T. R. Malthus, "An essay on the principle of population (1798)," *The Works of Thomas Robert Malthus, London, Pickering & Chatto Publishers*, vol. 1, pp. 1–139, 1986.

[12] B. Gompertz, "XXIV. On the nature of the function expressive of the law of human mortality, and on a new mode of determining the value of life contingencies. In a letter to Francis Baily, Esq. FRS &c," *Philosophical transactions of the Royal Society of London*, no. 115, pp. 513–583, 1825.

[13] W. O. Kermack and A. G. McKendrick, "A contribution to the mathematical theory of epidemics," *Proceedings of the royal society of london. Series A, Containing papers of a mathematical and physical character*, vol. 115, no. 772, pp. 700–721, 1927.

[14] S. Odatalla, "Stochastic Modeling of Zoonotic Disease," 2020.

[15] F. Brauer, "Mathematical epidemiology: Past, present, and future," *Infectious Disease Modelling*, vol. 2, no. 2, pp. 113–127, 2017.

[16] M. J. Keeling and P. Rohani, *Modeling infectious diseases in humans and animals*. Princeton university press, 2011.

[17] A. Afzal, C. A. Saleel, S. Bhattacharyya, N. Satish, O. D. Samuel, and I. A. Badruddin, "Merits and limitations of mathematical modeling and computational simulations in mitigation of COVID-19 pandemic: A comprehensive review," *Archives of Computational Methods in Engineering*, vol. 29, no. 2, pp. 1311–1337, 2022.

[18] B. Pike, K. Saylors, J. Fair, M. LeBreton, U. Tamoufe, C. Djoko, A. Rimoin, and N. Wolfe, "The origin and prevention of pandemics," *Clinical infectious diseases : an official publication of the Infectious Diseases Society of America*, vol. 50, pp. 1636–40, 06 2010.

[19] K. A. Alexander, B. L. Lewis, M. Marathe, S. Eubank, and J. K. Blackburn, "Modeling of wildlife-associated zoonoses: applications and caveats," *Vector-borne and zoonotic diseases*, vol. 12, no. 12, pp. 1005–1018, 2012.

[20] M. E. Cobos, A. T. Peterson, N. Barve, and L. Osorio-Olvera, "kuenm: an r package for detailed development of ecological niche models using maxent," *PeerJ*, vol. 7, p. e6281, 2019.

[21] T. J. Lawrence, B. P. Takenaka, A. Garg, D. Tao, S. L. Deem, E. M. Fèvre, I. Gluecks, V. Sagan, and E. Shacham, "A global examination of ecological niche modeling to predict emerging infectious diseases: a systematic review," *Frontiers in Public Health*, vol. 11, p. 1244084, 2023.

[22] X. Li, X. Wei, W. Yin, R. J. Soares Magalhaes, Y. Xu, L. Wen, H. Peng, Q. Qian, H. Sun, and W. Zhang, "Using ecological niche modeling to predict the potential distribution of scrub typhus in Fujian Province, China," *Parasites & Vectors*, vol. 16, no. 1, p. 44, 2023.

[23] L. Nyakarahuka, S. Ayebare, G. Mosomtai, C. Kankya, J. Lutwama, F. N. Mwiine, and E. Skjerve, "Ecological niche modeling for filoviruses: a risk map for Ebola and Marburg virus disease outbreaks in Uganda," *PLoS currents*, vol. 9, 2017.

[24] M. Xu, C. Cao, Q. Li, P. Jia, and J. Zhao, "Ecological niche modeling of risk factors for H7N9 human infection in China," *International journal of environmental research and public health*, vol. 13, no. 6, p. 600, 2016.

[25] S. P. Beeman, A. M. Morrison, T. R. Unnasch, and R. S. Unnasch, "Ensemble ecological niche modeling of West Nile virus probability in Florida," *Plos one*, vol. 16, no. 10, p. e0256868, 2021.

[26] A. Assefa, A. Tibebu, A. Bihon, A. Dagnachew, and Y. Muktar, "Ecological niche modeling predicting the potential distribution of African horse sickness virus from 2020 to 2060," *Scientific reports*, vol. 12, no. 1, p. 1748, 2022.

[27] R. H. Miller, P. Masuoka, T. A. Klein, H.-C. Kim, T. Somer, and J. Grieco, "Ecological niche modeling to estimate the distribution of Japanese encephalitis virus in Asia," *PLoS neglected tropical diseases*, vol. 6, no. 6, p. e1678, 2012.

[28] Q. Li, H. Ren, L. Zheng, W. Cao, A. Zhang, D. Zhuang, L. Lu, and H. Jiang, "Ecological niche modeling identifies fine-scale areas at high risk of dengue fever in the Pearl River Delta, China," *International Journal of Environmental Research and Public Health*, vol. 14, no. 6, p. 619, 2017.

[29] B. P. Monroe, Y. J. Nakazawa, M. G. Reynolds, and D. S. Carroll, "Estimating the geographic distribution of human Tanapox and potential reservoirs using ecological niche modeling," *International journal of health geographics*, vol. 13, pp. 1–9, 2014.

[30] M. F. Sallam, R.-D. Xue, R. M. Pereira, and P. G. Koehler, "Ecological niche modeling of mosquito vectors of West Nile virus in St. John's County, Florida, USA," *Parasites & Vectors*, vol. 9, pp. 1–14, 2016.

[31] R. Richman, D. Diallo, M. Diallo, A. A. Sall, O. Faye, C. T. Diagne, I. Dia, S. C. Weaver, K. A. Hanley, and M. Buenemann, "Ecological niche modeling of Aedes mosquito vectors of chikungunya virus in southeastern Senegal," *Parasites & vectors*, vol. 11, pp. 1–17, 2018.

[32] H. Choi and D.-I. Park, "A Patch Model for Pandemic Influenza Simulation in Korea," in *2010 Sixth IEEE International Conference on e-Science Workshops*, pp. 65–71, IEEE, 2010.

[33] J. Rebaza, "A general multipatch model of ebola dynamics," *Nonautonomous Dynamical Systems*, vol. 8, no. 1, pp. 125–135, 2021.

[34] J. Zhang, Z. Jin, H. Zhu, J. Zhang, Z. Jin, and H. Zhu, "Birds movement impact on the transmission of West Nile virus between patches," *J. Appl. Anal. Comput*, vol. 8, pp. 443–456, 2018.

[35] J. Chen, L. Zou, Z. Jin, and S. Ruan, "Modeling the geographic spread of rabies in China," *PLoS neglected tropical diseases*, vol. 9, no. 5, p. e0003772, 2015.

[36] M. Maliyoni, H. D. Gaff, K. S. Govinder, and F. Chirove, "Multipatch stochastic epidemic model for the dynamics of a tick-borne disease," *Frontiers in applied mathematics and statistics*, vol. 9, p. 1122410, 2023.

[37] M. J. Wonham, T. de Camino-Beck, and M. A. Lewis, "An epidemiological model for West Nile virus: invasion analysis and control applications," *Proceedings of the royal society of London. Series B: Biological Sciences*, vol. 271, no. 1538, pp. 501–507, 2004.

[38] C. Bekoe, "The sir model and the 2014 ebola virus disease outbreak in guinea, liberia and sierra leone," *Int. J. Appl. Sci*, vol. 6, no. 2, pp. 11–24, 2015.

[39] E. K. Lee, Y. Liu, and F. H. Pietz, "A compartmental model for Zika virus with dynamic human and vector populations," in *AMIA Annual Symposium Proceedings*, vol. 2016, p. 743, American Medical Informatics Association, 2016.

[40] M. L. Danzetta, R. Bruno, F. Sauro, L. Savini, and P. Calistri, "Rift Valley fever transmission dynamics described by compartmental models," *Preventive veterinary medicine*, vol. 134, pp. 197–210, 2016.

[41] A. Malek and A. Hoque, "Mathematical modeling of bird flu with vaccination and treatment for the poultry farms," *Comparative Immunology, Microbiology and Infectious Diseases*, vol. 80, p. 101721, 2022.

[42] S. Stiner and V. Chellamuthu, "An Agent-Based Model of West Nile Virus: Predicting the Impact of Public Health Agents and Vaccinations on Horses," *Curiosity: Interdisciplinary Journal of Research and Innovation*, vol. 2, pp. 44–66, 2020.

[43] C. Siettos, C. Anastassopoulou, L. Russo, C. Grigoras, and E. Mylonakis, "Modeling the 2014 ebola virus epidemic–agent-based simulations, temporal analysis and future predictions for liberia and sierra leone," *PLoS currents*, vol. 7, 2015.

[44] C. J. Kuhlman, Y. Ren, B. Lewis, and J. Schlitt, "Hybrid Agent-based modeling of Zika in the United States," in *2017 Winter Simulation Conference (WSC)*, pp. 1085–1096, IEEE, 2017.

[45] D. M. Nguyen, H. Deguchi, and M. Ichikawa, "Agent-based simulation on avian influenza in Vietnam: Basic characteristics of the epidemic and efficiency evaluation of control measures," in *2010 7th International Conference on Service Systems and Service Management*, pp. 1–6, IEEE, 2010.

[46] L. Huang, Y. Huang, Q. Wang, N. Xiao, D. Yi, W. Yu, and D. Qiu, "An agent-based model for control strategies of Echinococcus granulosus," *Veterinary parasitology*, vol. 179, no. 1-3, pp. 84–91, 2011.

[47] M. J. Keeling and K. T. Eames, "Networks and epidemic models," *Journal of the royal society interface*, vol. 2, no. 4, pp. 295–307, 2005.

[48] F. Brauer, "An introduction to networks in epidemic modeling," *Mathematical epidemiology*, pp. 133–146, 2008.

[49] F. D. Sahneh, C. Scoglio, and P. Van Mieghem, "Generalized epidemic mean-field model for spreading processes over multilayer complex networks," *IEEE/ACM Transactions on Networking*, vol. 21, no. 5, pp. 1609–1620, 2013.

[50] F. D. Sahneh, A. Vajdi, H. Shakeri, F. Fan, and C. Scoglio, "GEMFsim: A stochastic simulator for the generalized epidemic modeling framework," *Journal of computational science*, vol. 22, pp. 36–44, 2017.

[51] S. A. Moon, L. W. Cohnstaedt, D. S. McVey, and C. M. Scoglio, "A spatio-temporal individual-based network framework for West Nile virus in the USA: Spreading pattern of West Nile virus," *PLoS computational biology*, vol. 15, no. 3, p. e1006875, 2019.

[52] C. Ji and D. Jiang, "Threshold behaviour of a stochastic SIR model," *Applied Mathematical Modelling*, vol. 38, no. 21-22, pp. 5067–5079, 2014.

[53] F. Brauer, "Compartmental models in epidemiology," *Mathematical epidemiology*, pp. 19–79, 2008.

[54] S. Bansal, B. T. Grenfell, and L. A. Meyers, "When individual behaviour matters: homogeneous and network models in epidemiology," *Journal of the Royal Society Interface*, vol. 4, no. 16, pp. 879–891, 2007.

[55] B. Wang, G. Tanaka, H. Suzuki, and K. Aihara, "Epidemic spread on interconnected metapopulation networks," *Physical Review E*, vol. 90, no. 3, p. 032806, 2014.

[56] Y. Wang and G. Xiao, "Effects of interconnections on epidemics in network of networks," in *2011 7th International Conference on Wireless Communications, Networking and Mobile Computing*, pp. 1–4, IEEE, 2011.

[57] F. D. Sahneh, C. Scoglio, and F. N. Chowdhury, "Effect of coupling on the epidemic threshold in interconnected complex networks: A spectral analysis," in *2013 American control conference*, pp. 2307–2312, IEEE, 2013.

[58] G. Bianconi, *Multilayer networks: structure and function*. Oxford university press, 2018.

[59] J. Gao, A. Bashan, L. Shekhtman, and S. Havlin, *Introduction to Networks of Networks*. IOP Publishing, 2022.

[60] G. D'Agostino and A. Scala, *Networks of networks: the last frontier of complexity*, vol. 340. Springer, 2014.

[61] L. M. Shekhtman, M. M. Danziger, and S. Havlin, "Spreading of failures in interdependent networks," in *Diffusive spreading in nature, technology and society*, pp. 389–403, Springer, 2023.

[62] H. Sanhedrai, J. Gao, A. Bashan, M. Schwartz, S. Havlin, and B. Barzel, "Reviving a failed network through microscopic interventions," *Nature Physics*, vol. 18, no. 3, pp. 338–349, 2022.

[63] F. Radicchi and A. Arenas, "Abrupt transition in the structural formation of interconnected networks," *Nature Physics*, vol. 9, no. 11, pp. 717–720, 2013.

[64] H. Wang, Q. Li, G. D'Agostino, S. Havlin, H. E. Stanley, and P. Van Mieghem, "Effect of the interconnected network structure on the epidemic threshold," *Physical Review E*, vol. 88, no. 2, p. 022801, 2013.

[65] G. Zhu, X. Fu, Q. Tang, and K. Li, "Mean-field modeling approach for understanding epidemic dynamics in interconnected networks," *Chaos, Solitons & Fractals*, vol. 80, pp. 117–124, 2015.

[66] Y. Wang and G. Xiao, "Epidemics spreading in interconnected complex networks," *Physics Letters A*, vol. 376, no. 42-43, pp. 2689–2696, 2012.

[67] M. Dickison, S. Havlin, and H. E. Stanley, "Epidemics on interconnected networks," *Physical Review E*, vol. 85, no. 6, p. 066109, 2012.

[68] J. Jia, Z. Jin, and X. Fu, "Epidemic spread in directed interconnected networks," *Communications in Nonlinear Science and Numerical Simulation*, vol. 75, pp. 1–13, 2019.

[69] Z. Xu, Y. Wang, N. Wu, and X. Fu, "Propagation dynamics of a periodic epidemic model on weighted interconnected networks," *IEEE Transactions on Network Science and Engineering*, vol. 7, no. 3, pp. 1545–1556, 2019.

[70] A. Nandi and L. J. Allen, "Probability of a zoonotic spillover with seasonal variation," *Infectious Disease Modelling*, vol. 6, pp. 514–531, 2021.

[71] Z. L. Grange, T. Goldstein, C. K. Johnson, S. Anthony, K. Gilardi, P. Daszak, K. J. Olival, T. O'Rourke, S. Murray, S. H. Olson, *et al.*, "Ranking the risk of animal-to-human spillover for newly discovered

viruses," *Proceedings of the National Academy of Sciences*, vol. 118, no. 15, p. e2002324118, 2021.

[72] J. H. Ellwanger and J. A. B. Chies, "Zoonotic spillover: Understanding basic aspects for better prevention," *Genetics and Molecular Biology*, vol. 44, 2021.

[73] K. Royce and F. Fu, "Mathematically modeling spillovers of an emerging infectious zoonosis with an intermediate host," *PloS one*, vol. 15, no. 8, p. e0237780, 2020.

[74] R. K. Plowright, C. R. Parrish, H. McCallum, P. J. Hudson, A. I. Ko, A. L. Graham, and J. O. Lloyd-Smith, "Pathways to zoonotic spillover," *Nature Reviews Microbiology*, vol. 15, no. 8, pp. 502–510, 2017.

[75] E. M. Rees, A. Minter, W. J. Edmunds, C. L. Lau, A. J. Kucharski, and R. Lowe, "Transmission modelling of environmentally persistent zoonotic diseases: a systematic review," *The Lancet Planetary Health*, vol. 5, no. 7, pp. e466–e478, 2021.

[76] S. Dutta and U. Ray, "Paratracheal abscess by plant fungus Chondrostereum purpureum-first case report of human infection," *Medical Mycology Case Reports*, vol. 40, pp. 30–32, 2023.

[77] M. Youssef and C. Scoglio, "An individual-based approach to SIR epidemics in contact networks," *Journal of theoretical biology*, vol. 283, no. 1, pp. 136–144, 2011.

[78] R. A. Horn and C. R. Johnson, *Matrix analysis*. Cambridge University Press, 2012.

[79] D. J. Watts and S. H. Strogatz, "Collective dynamics of 'small-world'networks," *nature*, vol. 393, no. 6684, pp. 440–442, 1998.

[80] P. Erdős, A. Rényi, *et al.*, "On the evolution of random graphs," *Publ. Math. Inst. Hung. Acad. Sci*, vol. 5, no. 1, pp. 17–60, 1960.

[81] S. J. Salyer, R. Silver, K. Simone, and C. B. Behravesh, "Prioritizing zoonoses for global health capacity building—themes from One Health zoonotic disease workshops in 7 countries, 2014–2016," *Emerging infectious diseases*, vol. 23, no. Suppl 1, p. S55, 2017.

[82] R. Sahu, D. P. Das, and S. Nayak, "Emergence of zoonoses at human-animal interface," *Int. J. Curr. Microbiol. Appl. Sci*, vol. 9, pp. 2894–2905, 2021.

[83] G. Machado and G. Baxter, "Effect of initial infection size on a network susceptible-infected-recovered model," *Physical Review E*, vol. 106, no. 1, p. 014307, 2022.

[84] H. Andersson and T. Britton, *Stochastic epidemic models and their statistical analysis*, vol. 151. Springer Science & Business Media, 2012.

[85] S. Hosseini, L. W. Cohnstaedt, J. M. Humphreys, and C. Scoglio, "A Parsimonious Bayesian Predictive Model for Forecasting New Reported Cases of West Nile Disease," *Infectious Disease Modelling*, 2024.

[86] E. F. S. A. (EFSA), A. Brouwer, J. Gonzales, A. Huneau, P. Mulatti, T. Kuiken, C. Staubach, A. Stegeman, S.-E. Antoniou, F. Baldinelli, *et al.*, "Annual Report on surveillance for avian influenza in poultry and wild birds in Member States of the European Union in 2018," *EFSA Journal*, vol. 17, no. 12, p. e05945, 2019.

[87] M. R. Gomaa, A. S. Kayed, M. A. Elabd, D. A. Zeid, S. A. Zaki, A. S. El Rifay, L. S. Sherif, P. P. McKenzie, R. G. Webster, R. J. Webby, *et al.*, "Avian influenza A (H5N1) and A (H9N2) seroprevalence and risk factors for infection among Egyptians: a prospective, controlled seroepidemiological study," *The Journal of Infectious Diseases*, vol. 211, no. 9, pp. 1399–1407, 2015.

[88] E. C. f. D. P. European Food Safety Authority, E. U. R. L. f. A. I. Control, C. Adlhoch, A. Fusaro, J. L. Gonzales, T. Kuiken, S. Marangon, É. Niqueux, C. Staubach, C. Terregino, I. Aznar, *et al.*, "Avian influenza overview September–December 2022," *EFSA Journal*, vol. 21, no. 1, p. e07786, 2023.

[89] A.-L. Barabási and E. Bonabeau, "Scale-free networks," *Scientific american*, vol. 288, no. 5, pp. 60–69, 2003.

[90] M. Liu, D. Li, P. Qin, C. Liu, H. Wang, and F. Wang, "Epidemics in interconnected small-world networks," *PloS one*, vol. 10, no. 3, p. e0120701, 2015.

[91] J. M. Drake, I. Bakach, M. R. Just, S. M. O'Regan, M. Gambhir, and I. C.-H. Fung, "Transmission models of historical Ebola outbreaks," *Emerging infectious diseases*, vol. 21, no. 8, p. 1447, 2015.